Flinders
UNIVERSITY

Sediment mobilisation and release through groundwater discharge to the land surface: Review and theoretical development

Abstract

The discharge of groundwater to the land surface and to lakes and streams may express subsurface particles. This may lead to preferential pathways and increased fluxes of groundwater, sediment and contaminants, and modified subsurface structures. The current review attempts to describe and categorise the various forms through which sediment may be liberated in areas of groundwater discharge. Forces acting on subsurface particles in areas of groundwater discharge include seepage (drag), buoyancy and particle weight, amongst other, more complex forces. Equations for these can be combined to create formulae for approximating the conditions under which groundwater discharge will transport particles to the surface. Two forms of subsurface sediment transport are considered: (1) flow through an immobile granular matrix (*suffusion* and *suffosion*), and (2) flow through preferential pathways (i.e., often treated as pipes). Suffusion involves sediment movement that does not impact the soil's stability, whereas suffosion creates changes to soil stability and, consequently, soil volume. Preferential flow may arise from cracks in cohesive materials or through localised fluidization of non-cohesive soils, leading in some situations to *sand boils*. Guidance is presented on the minimum theoretical hydraulic gradient required for grains of various sizes to start to rise. New simple formulae are developed that build on existing theory, and these are compared to previous laboratory data, showing that suffusion is more or less predictable using the new simple method. However, experimental sand boils require larger hydraulic gradients compared to theory. The current analysis summarises the state of knowledge and persistent knowledge gaps associated with sediment ejection through groundwater discharge, which we

26 expect has wide-ranging applications in terms of sediment transport in coastal regions and to
27 surface water bodies, and where strong groundwater discharge is known to occur.

1. Introduction

The expression of groundwater at the land surface is a common occurrence. Groundwater discharge (or *seepage flow*) is critical to the survival of ecosystems in water-limited regions and provides significant fluxes of dissolved chemicals to surface water bodies, including the ocean (e.g., Moore, 2010). In some situations, seepage flows may also entrain subsurface particles and transport these to the surface and/or surface water bodies.

The transport of particles by groundwater has received considerable attention in the field of dam safety, because the failure of earth dams may initially present as ejected subsurface particles in groundwater discharge zones (van Beek et al., 2013). Particle displacement below dam structures may be initiated where the friction forces arising from flowing groundwater are sufficient to rotate, dislodge and mobilise sediment particles (e.g., Sellmeijer, 1988; van Beek et al., 2013). *Piping* was described by Hagerty (1991) as the removal of particles by seepage outflow that forms cylindrical conduits commonly conceptualised as pipes. If seepage exfiltration occurs in a larger area, the term *sapping* can be used (Jones, 1981; Hagerty, 1991). Sapping has the same characteristics as piping in that both are particle removal mechanisms resulting in pipe formation, except that with sapping larger lenticular cavities can also appear (Hagerty, 1992). Additionally, the term *jugging* has also been used to describe vertical erosion tunnels (Decker and Dunnigan, 1977). Richards and Reddy (2007) acknowledged that jugging in dispersive soils is caused by rainfall erosion and might lead to dam failures that resemble erosion originated by animals or tree roots.

Where sediment is subsequently transported downstream of an engineering structure, hollow spaces in or underneath dam structures can grow in the opposite direction of the flow,

potentially leading to *piping failure* (van Beek et al., 2013), including such catastrophic events as the collapse of the Teton Dam (USA) in 1976 (Jones, 1981; Richards and Reddy, 2007). The various forms of sediment movement in the vicinity of engineering structures is termed *internal erosion* by FEMA (2015). *Contact erosion* and *concentrated leak erosion* are also internal erosion mechanisms. The former can occur where coarse and fine soils are in contact and there is a flow parallel to the contact, leading to erosion of the finer soil (Bonelli and Nicot, 2013). Concentrated leak erosion takes place through cracks originated by hydraulic fractures due to, for example, differential settlement during construction of a dam or levee (Bonelli et al., 2013). Another phenomenon commonly related to subsurface erosion is the *sand boil*, which may appear, often in groups, in areas of groundwater discharge. These typically appear as small, volcano-shaped vents through which sediment is released, and have been observed downstream of water-retaining structures (e.g., dams, dikes, etc.; TACFD, 1999). Artificial sand boils have been created in laboratory experiments (Miesel, 1978; Muller-Kirchenbauer, 1978) and in field-scale experiments (Silvis, 1991; van Beek et al., 2011) to study the erosion of levees.

Sediment may also be liberated from the subsurface in the absence of surface water impoundments. For example, de Louw et al. (2010, 2013) observed preferential groundwater flow in the form of localised expressions of upwelling groundwater (i.e., *boils*) or as larger vents with both water and sediment discharge (i.e., sand boils) in Dutch polders. They attributed these and similar features in other Dutch polders to the considerable groundwater hydraulic gradients that arise from the low land surface elevation, relative to sea level, of much of The Netherlands. De Louw et al. (2010, 2013) suggest that the boils and sand boils in Dutch polders arise after cohesive layers heave, leading to preferential pathways through which groundwater flows at high velocities. Sand boils were particularly evident beneath lower polders. Sand boils have also been observed in river embankments, for example, during floods

78 in: the Rhine, Waal, IJssel and Maas Rivers (The Netherlands; van Beek et al., 2013), the
79 Yangtze and Nenjiang Rivers (China; Yao et al., 2009), and the Mississippi River (USA; Li et
80 al., 1996; Mansur et al., 2000; Glynn and Kuszmaul, 2010).
81
82 The current review evaluates the liberation of subsurface particles under the action of vertical
83 groundwater flow, regardless of whether the situation is natural or engineered, although our
84 primary focus is that of natural conditions. The flow pathways through which subsurface
85 particles may be transported vertically to the land surface can be divided into two categories:
86 (1) flow through immobile pore networks within a granular matrix, and (2) flow through
87 preferential pathways. The latter may arise from cracks in cohesive materials, through localised
88 fluidity of non-cohesive soils (i.e., in which gravity, buoyancy effects and drag from flowing
89 groundwater control intergranular forces) or through pathways created from more natural
90 processes such as desiccation cracking, root holes, rodent activity and anthropogenic causes.
91 In (1), the particles transported through a pore network by groundwater flow must be small
92 enough to pass through the intergranular spaces, and groundwater flow must be strong enough
93 to erode particles and transport them upwards against the submerged gravitational force (i.e.,
94 sediment weight minus buoyancy) acting on each particle. In (2), hydraulic forces must be large
95 enough to cause heave (i.e., uplift) of cohesive layers and/or sand fluidization, and to transport
96 particles upwards against submerged gravitational forces. Figure 1 provides a schematic
97 illustration of conceptual models for the different forms of subsurface sediment transport that
98 lead to the ejection of particles.
99

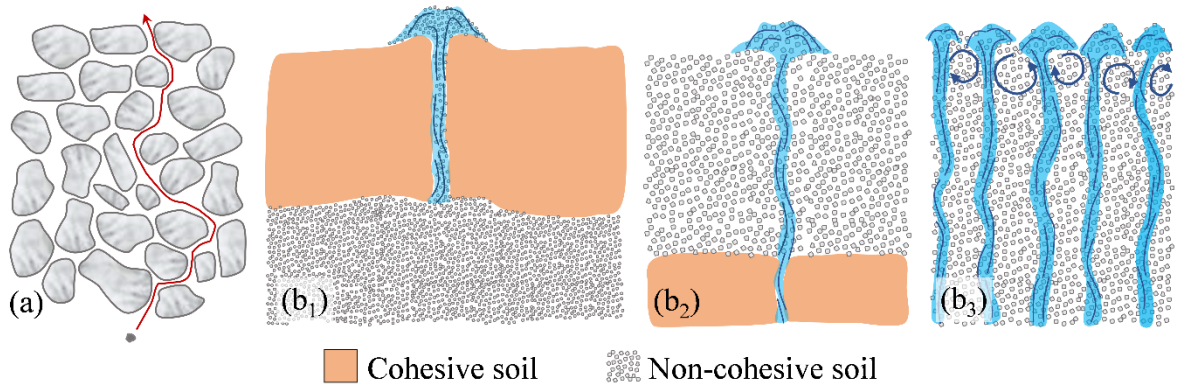

Figure 1. Schematic illustration of different forms of subsurface sediment transport: (a) the passage of small particles through immobile pore networks (*suffusion* and *suffosion*), (b) three forms of sediment transport through preferential pathways. Two types of *sand boils* are shown: (b_1) preferential flow through a cohesive soil layer leading to the vertical transport of particles from the underlying non-cohesive sediment body, and (b_2) preferential flow within a non-cohesive soil layer caused by localised discharge from below (e.g., due to a fault or fracture). At sufficiently high hydraulic gradients, widespread fluidisation may cause (b_3) *boiling sand*.

The theory developed in this research is an extension to previous studies of vertical sediment transport in the subsurface because we consider relationships between sediment particle characteristics and hydraulic forces for various forms of sediment transport through porous media. While prior studies mainly focus on specific conditions, the current research aims to review theoretical bases for estimating vertical particle displacement under various common mechanisms and situations.

2. Theory

2.1 Particle movement under vertical fluid flow

Here, we consider the forces acting on a single particle within a moving fluid body. A single particle in a stationary fluid will eventually descend at its terminal velocity (V_T), whereby the total resistance force or drag force (F_D) becomes equal to the difference between the particle's weight (W) and the buoyancy force (F_B) acting on it, as (Prandtl and Tietjens, 1934):

$$F_D = C_D A_P \frac{\rho_f V_T^{\,2}}{2} = W - F_B \quad (1)$$

where C_D is the drag coefficient, A_P is the projected area of the particle and ρ_f is the fluid density. C_D can be expressed as a function of Reynolds number (Re) and the shape of the particle (e.g., Madhav and Chhabra, 1995), where Re is given by:

$$Re = \frac{\rho_f U L}{\mu} \quad (2)$$

Here, U is the velocity (taken as the terminal velocity of the particle, V_T), L is the characteristic dimension (taken as the particle diameter, d) and μ is the dynamic viscosity of the fluid (approximately 10^{-3} Pa.s for freshwater). Alternative forms of equation (2) apply to different situations of subsurface sediment movement, as addressed in subsequent sub-sections. At small Re (less than 0.5), two-thirds of the total resistance to flow around spheres is due to shear (friction drag) and one-third is due to pressure (form drag) (Lamb, 1932). Stokes' law can be used to define C_D for $Re < 0.5$, e.g., for spheres (e.g., Clift et al., 1978):

$$C_D = \frac{24}{Re} \quad (3)$$

The corresponding Stokes' terminal velocity (V_{ST}) (i.e., for the submerged descent on a single particle) can be calculated by combining equations (1) and (3), as (e.g., Clift et al., 1978):

142 $$V_{ST} = \frac{1}{18}\frac{(\rho_s - \rho_f)}{\mu} g d^2 \quad (4)$$

143

144 Here, ρ_s is the particle density, and g is gravity (taken as 9.8 m/s^2). Table 1 summarises V_{ST} and
145 Re for different particle sizes using equations (4) and (2), respectively. It is assumed that
146 particles are spherical, and that ρ_s and ρ_f are 2650 kg/m^3 (i.e., approximately that of quartz sand
147 grains) and 1000 kg/m^3, respectively.

148

149 **Table 1.** Stokes' terminal velocity and corresponding Reynolds number for different particle
150 sizes. Particle sizes are the limits for each particle description (for example, medium sand
151 falls within the range 0.25 to 0.5 mm) following the Wentworth (1922) scale.

Particle description	Particle size, d (mm)	Stokes' terminal velocity, V_{ST} (m/s)	Re	Stokes' law validity
Very coarse sand	2	3.6	7191	Not valid
	1	0.90	899	Not valid
Coarse sand				
	0.5	0.22	112	Not valid
Medium sand				
	0.25	0.056	14	Not valid
Fine sand				
	0.125	0.014	1.76	Not valid
Very fine sand				
	0.0625	0.0035	0.22	Valid

152

153 Combining equations (2) and (4), it can be shown that C_D calculated using equation (3) is not
154 valid for d > 0.0625mm (i.e., sediment larger than very fine sand; Table 1). Hence, other
155 relationships need to be used for fine sand (or larger) grains to obtain C_D. Tran-Cong et al.
156 (2004) developed an empirical function to calculate C_D for irregularly shaped particles. Their
157 formulation is based on Re and the geometric characteristics of the particle, as:

158 $$C_D = \frac{24}{Re}\frac{d_A}{d_n}\left[1+\frac{0.15}{\sqrt{c}}\left(\frac{d_A}{d_n}Re\right)^{0.687}\right]+\frac{0.42\left(\frac{d_A}{d_n}\right)^2}{\sqrt{c}\left[1+4.25\times10^4\left(\frac{d_A}{d_n}Re\right)^{-1.16}\right]} \quad (5)$$

159

160 Here, d_n is the diameter of a sphere of equal volume to the particle (e.g., Wadell, 1933), d_A is
161 the diameter of a sphere of equal projected surface area (i.e., perpendicular to the flow
162 direction) to the particle (e.g., Heywood, 1962), and c is the particle circularity or surface
163 sphericity, given by $c = \pi d_A / P_P$, where P_P is the perimeter of the projected surface area of the
164 particle (e.g., Wadell, 1933). Equation (5) is valid for $0.15 < Re < 1500$, $0.80 < d_A/d_n < 1.50$
165 and $0.4 < c < 1.0$, which covers most irregularly shaped particles in practical applications (Tran-
166 Cong et al., 2004). For spherical particles, d_A/d_n and c are 1, and equation (5) reduces to the
167 expression for spheres derived by Clift et al. (1978).

168

169 By rearranging equation (1), V_T can be calculated by:

170 $$V_T = \sqrt{\frac{2F_D}{C_D A_P \rho_f}} = \sqrt{\frac{2(W-F_B)}{C_D A_P \rho_f}} \quad (6)$$

171

172 Equation (6) needs to be solved iteratively because C_D is a function of Re (equation (5)),
173 which is a function of V_T (equation (2)).

174

175 As an alternative to the previous methodology for estimating the terminal velocity, Gibbs et
176 al. (1971) derived an empirical equation for the relationship between V_T and d for spherical
177 particles of diameters ranging from 0.1 μm to 6 mm, as:

178 $$V_T = \frac{-3\mu+\sqrt{9\mu^2+gd^2\rho_f(\rho_s-\rho_f)(3.869\times10^{-5}+2.48\times10^{-2}d)}}{\rho_f(1.1607\times10^{-4}+7.4405\times10^{-2}d)} \quad (7)$$

Table 2 shows V_T values calculated using equations (6) and (7) for spherical sand grains (using values for ρ_s, ρ_f and μ as defined above). The comparison shows good agreement (less than 8% difference) between V_T values obtained using the two alternative methods. Comparison to Table 1 shows the order-of-magnitude error that arises if Stokes' terminal velocity is applied to larger particles.

Table 2. Terminal velocity of different sizes of spherical sand grains in freshwater.

Particle description	Particle size, d (mm)	Gibbs et al. (1971)	Tran-Cong et al. (2004)		
		Terminal velocity, V_T (m/s) (eq. (7))	Terminal velocity, V_T (m/s) (eq. (6))	*Re*	Drag coefficient, C_D (eq. (5))
Very coarse sand	2	0.27	0.28	558	0.56
	1	0.15	0.16	155	0.90
Coarse sand	0.5	0.076	0.078	39	1.8
Medium sand	0.25	0.032	0.034	8.5	4.7
Fine Sand	0.125	0.011	0.012	1.5	20
Very fine sand	0.0625	0.0033	0.0034	0.21	120

2.2 Sediment transport through immobile pore networks (suffusion)

Water moving through a porous medium (i.e., seepage flow) creates dynamic forces on particles. If these forces exceed stabilizing forces holding particles in position, they may be mobilized. Some particles dislodged in this way may be small enough to pass through the pore network of the body of sediment; a phenomenon referred to as *seepage-induced internal instability* (Fannin and Slangen, 2014). The pathway of moving particles is determined by the internal structure of the porous medium and the direction of groundwater flow (Kovacs, 1981).

196 Fannin and Slangen (2014) reviewed various terms and descriptions of seepage-induced
197 internal instability phenomena used in the literature. Fannin and Slangen (2014) suggested that
198 different seepage-induced internal instability phenomena can be characterised and
199 distinguished based on measuring three variables including changes in the mass, volume and
200 hydraulic conductivity (*K*) of the porous medium. The latter can be deducted from
201 measurements of flow rates and hydraulic gradients which are commonly recorded in
202 experimental studies (e.g., Skempton and Brogan, 1994; Wan and Fell, 2004; Moffat et al.,
203 2011).
204
205 The stability of the porous medium skeleton may be modified depending on the rate of particle
206 movement and the role of small particles in the mechanical strength of the soil. Accordingly,
207 Fannin and Slangen (2014) recommended the term *"suffusion"* to describe "the non-
208 destructive response, which may be quantified by a mass loss, no change in volume and an
209 increase in hydraulic conductivity." They also advocated the term "*suffosion"* to describe "the
210 instability phenomenon whereby the transport of fine particles by seepage flow is accompanied
211 by a collapse of the soil structure." In other words, suffusion involves fine particle transport by
212 seepage flow, resulting in mass reduction and an increase in *K*, while the volume of porous
213 medium is not changed and the stability of the skeleton composed by the coarse grains is
214 unaffected. Suffusion becomes *suffosion* if the migration of fine particles affects the porous
215 medium skeleton (i.e., through rearrangement of coarser grains), resulting in an overall change
216 to the soil body stability and a reduction in the solid volume accompanied by changes in *K*
217 (Fannin and Slangen, 2014).
218
219 For suffusion to occur, Fell and Fry (2013) proposed three criteria: (1) geometric criterion, (2)
220 stress criterion, and (3) hydraulic criterion. The geometric criterion is a prerequisite that

identifies that the pore size must be large enough to allow fine particles to pass through. The stress criterion establishes that the amount of finer particles must be less than enough to fill the voids of the soil matrix formed by the coarser particles, allowing free movement to some of finer particles in the soil matrix. For the hydraulic criterion to be satisfied, the flow velocity must be high enough to move fine particles through granular pore spaces. Significant research has been undertaken into the internal stability of soils from the geometric point of view (e.g., Kenney and Lau, 1985; Fannin and Moffat, 2006; Wan and Fell, 2008; Indraratna et al., 2011). Chang and Zhang (2013) summarized several existing geometric criteria in the literature and developed a dataset of soil internal stability tests. Here, soils that are *internally stable* have an ability to act as a filter thereby preventing the loss of small particles due to disturbing forces such as seepage and vibration (Kenney and Lau, 1985). Soils are otherwise considered *internally unstable* where suffusion may arise under the action of high groundwater flow. Factors such as clay dispersiveness may greatly enhance the susceptibility of soils to suffusion, particularly in engineered structures (FEMA, 2015). Transport and removal of finer individual particles may lead to micro-scale holes (e.g., de Wit et al., 1981; van Beek et al., 2011). Therefore, suffusion may be the first sign of increasing levels of internal erosion (van Beek et al., 2013), and is of interest in the design of filtration/drainage systems, particularly in relation to engineering structures that are vulnerable to piping failure (Worman and Olafsdottir, 1992).

Several numerical models have been developed to simulate seepage-induced fine particle transport through granular materials by coupling particle-based methods with groundwater flow modelling techniques (e.g., Abdelhamid and El Shamy, 2016; Cheng et al., 2018; Aboul Hosn et al., 2018). The flow of water through pores may be considered at the macroscopic level using continuum approaches or at a microscopic level where pore-scale flow is characterised, e.g., using discrete approaches such as the lattice Boltzmann method or the pseudo-particle

method (Zhou et al., 2010). In the following, theory relating granular pore space, flow velocities and sediment movement is reviewed and combined to develop simple relationships between typical subsurface conditions and the characteristics of particles likely to be ejected with groundwater discharge.

2.2.1 Host media characteristics

The minimum pore (cavity) width (d_P) of granular materials dictates the largest particle size that can pass through a porous medium, and therefore dictates whether suffusion will occur. The packing of particles is a significant factor in the value of d_P. Theoretically, there are five different ways to pack uniform spherical particles which are shown in Figure 2 (White and Walton, 1937).

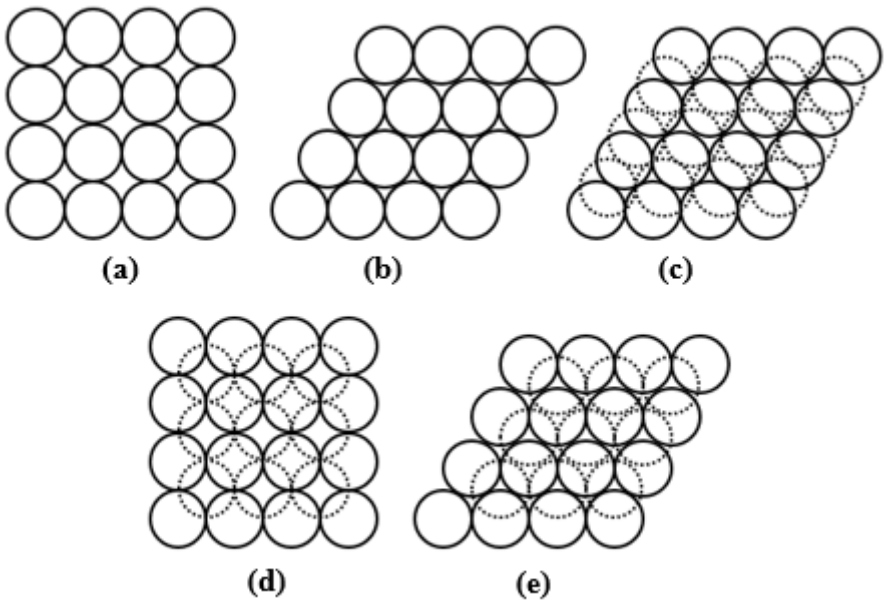

Figure 2. Different packing arrangements for uniform spherical particles: (a) Cubical, (b) Single-staggered (Orthorhombic), (c) Double-staggered (Tetragonal), (d) Pyramidal (Rhombohedral), (e) Tetrahedral (Rhombohedral). The solid circles represent spheres in one

plane, while the dotted ones indicate the spheres (that are obscured from view) in the next layer (White and Walton, 1937).

Table 3 lists d_P, the number of pathways (per particle) with pore width equal to d_P, and porosity (n). These can be calculated based on the geometric configuration of each packing arrangement (Gupta and Larson, 1979), noting that for some packing arrangements (e.g., double-staggered, pyramidal, tetrahedral) there are alternative values of d_P given in Table 3 due to different possible sub-configurations.

Table 3. Porosity, minimum pore (cavity) width and number of cavities (i.e., the number of void spaces adjacent to a particle with the same minimum pore size) in various packing arrangements for uniform spherical particles (Gupta and Larson, 1979). Note that (a) and (b) denote alternative values of d_P due to different possible sub-configurations.

Packing arrangement	Porosity, n	Minimum pore (cavity) width, d_P	No. of cavities	Stability
Cubical	0.48	0.732d	1	Unstable
Single-staggered (Orthorhombic)	0.40	0.531d	1	Unstable
Double-staggered (Tetragonal)	0.30	(a) 0.285d (b) 0.155d	2 4	Partially stable
Pyramidal (Rhombohedral)	0.26	(a) 0.414d (b) 0.225d	1 2	Completely stable
Tetrahedral (Rhombohedral)	0.26	(a) 0.414d (b) 0.225d	1 2	Completely stable

The pyramidal and tetrahedral arrangements of Table 3 are completely stable, whereas the double-staggered arrangement is partially stable requiring some support from the container walls. The cubical and single-staggered arrangements are unstable in that they need considerable support from the container walls (e.g., Graton and Fraser, 1935; Gray, 1968). In field and laboratory conditions, the formation of unstable packing arrangements in soil (i.e., cubical and single-staggered) is highly unlikely. Therefore, only completely stable (i.e.,

pyramidal and tetrahedral) and partially stable (i.e., double-staggered) arrangements are used in assigning minimum pore widths in the analysis that follows. While we consider idealised (uniform grain size) materials, natural granular materials will comprise grain size distributions that lead to pore sizes (and values of n) that are probably lower than those given in Table 3, because of pore-clogging by smaller particles. For example, the average pore size for well-sorted material was estimated by Sherard et al. (1984) as $0.11d_{15}$, where d_{15} is the equivalent particle size (diameter) at which 15% of the soil is finer by mass. However, in the absence of guidance on relationships between grain size distributions and d_P, we adopt the idealistic Table 3 values for the remainder of the analysis to demonstrate the development of theory.

We consider next the flow within sediments of known grain diameters (and therefore pore size), assuming relationships given in Table 3. The determination of flow in porous media requires knowledge of permeability (k), which can be approximated from d and n using empirical relationships such as Kozeny's (1927) permeability model, as:

$$k = c_0 \frac{d^2}{36} \frac{n^3}{(1-n)^2} \tag{8}$$

where c_0 is a constant that can vary from 1/2 (assuming capillary tubes have circular cross-sections) to 1/6 (Carman, 1937).

The relationships between pore size and packing arrangement in Table 3 are used to estimate pore sizes for typical grain diameters (assuming uniform particle size) in Table 4. We assume that Table 4 applies to materials with narrow ranges in particle sizes (i.e., uniformly graded or well-sorted sediments). Table 4 lists values of k and d_P (using equation (8) and assuming c_0 =

1/2) for different packing arrangements, where d_P corresponds with the standard grain sizes used in Table 2.

Table 4. Minimum pore widths, i.e., reflecting the maximum size of particles that may move through the host material, and the corresponding particle diameter of host material and the permeability for different packing arrangements.

Minimum pore width, d_P (mm)	Particle diameter (d) and permeability (k) of host material							
	Double-staggered (n = 0.30)				Pyramidal, Tetrahedral (n = 0.26)			
	$d = d_P/0.155$ (mm)	k (m^2)	$d = d_P/0.285$ (mm)	k (m^2)	$d = d_P/0.225$ (mm)	k (m^2)	$d = d_P/0.414$ (mm)	k (m^2)
2	12.9	1.31E-07	7.02	3.86E-08	8.89	3.50E-08	4.83	1.03E-08
1	6.45	3.26E-08	3.51	9.65E-09	4.44	8.74E-09	2.42	2.58E-09
0.5	3.23	8.16E-09	1.75	2.41E-09	2.22	2.19E-09	1.21	6.46E-10
0.25	1.61	2.04E-09	0.877	6.03E-10	1.11	5.46E-10	0.604	1.61E-10
0.125	0.806	5.10E-10	0.439	1.51E-10	0.556	1.37E-10	0.302	4.04E-11
0.0625	0.403	1.28E-10	0.219	3.77E-11	0.278	3.42E-11	0.151	1.01E-11

2.2.2 Initiation of suffusion: Critical flow velocity

The vertical movement of particles with sufficiently small diameter to pass through the pore network of a larger-diameter sediment is firstly examined by assuming that these particles will rise when the average interstitial velocity (V_G) is greater than V_T. The critical condition (i.e., when particles of diameter d_P become unstable) arises when V_G equals V_T. This requires the assumption that V_G is locally independent of pore sizes, and therefore, the resulting theory is an initial, macro-scale approximation. V_G can be estimated from known relationships between V_G and the groundwater hydraulic gradient (i). However, the relationship between i and V_G differs according to the flow conditions (i.e., laminar/Darcy, transitional or turbulent/non-Darcy) through porous media, which can be determined based on *Re* using equation (2). In applying equation (2) to determine *Re*, Bear (1972) suggested to adopt $U = q$, where q is the specific discharge or Darcy velocity, calculated as the product of n and V_G. Different parameters have been assigned to L (i.e., the representative dimension of moving particles) in

previous studies, including the mean grain diameter (d_m), other particle diameter statistics such as d_{10} or d_{50} (diameters at which 10% or 50% of a sample's mass is comprised of finer particles; Bear, 1972), $(k/n)^{1/2}$ (Collins, 1961) and $k^{1/2}$ (Ward, 1964). Various methods have been recommended for defining d_m, including that of Folk and Ward (1957), who suggest setting $\log_2 d_m = \log_2 d_{16} + \log_2 d_{50} + \log_2 d_{84}$.

Several values for *Re* at which flow transitions from laminar to turbulent (i.e., the critical *Re*; Re_c) are reported in the literature. Zeng and Grigg (2006) reviewed studies on non-Darcy (i.e., turbulent) flow behaviour in porous media and encountered ranges for Re_c that vary between that recommended by Bear (1972) (i.e., $1 < Re_c < 10$), and that of Fancher and Lewis (1933) (i.e., $10 < Re_c < 1000$).

The relation between i and V_G for different flow conditions in porous media is expressed by Bear (1972) as:

$$|i| = \begin{cases} q\dfrac{\mu}{k\rho_f g} & Re \le Re_c \text{ (Darcy/Laminar flow)} \\ aq + bq^2 & Re > Re_c \text{ (Non-Darcy/Turbulent flow)} \end{cases} \quad \text{where } q = nV_G \qquad (9)$$

Here, a and b are constants whose values have been obtained experimentally in numerous studies, as reviewed by Bear (1972). Equation (9) uses the absolute value of i to account for negative fluxes arising from positive values of i. In the current analysis, the equations provided by Ward (1964) are used to find a and b for non-Darcy flow in equation (9), as:

$$a = \frac{\mu}{k\rho_f g},\ b = \frac{0.55}{g\sqrt{k}} \qquad (10)$$

Application of equation (9) to values of V_T given in Table 2 (e.g., obtained from equation (6)) allows for an evaluation of the hydraulic gradient (i_{suf}) at which vertical suffusion (i.e., the vertical movement of subsurface particles) occurs, at least in terms of the largest particles that can pass through the porous matrix (i.e., of diameter d_P, see Table 3) and on the basis of other assumptions described above. Smaller particles will theoretically rise under hydraulic gradients less than i_{suf}, so that gradients greater than or equal to i_{suf} will theoretically cause suffusion of all non-cohesive sediment smaller than the minimum pore space of the immobile matrix. According to values for n and k in Table 4, i_{suf} (i.e., leading to $V_G = V_T$) for different packing arrangements is illustrated in Figure 3. To obtain the i_{suf} values in Figure 3, Re was first calculated using equation (2) (where $L = d$ and $U = q = nV_G$) for the combinations of d and n values given in Table 4 and assuming V_G equals the corresponding V_T values in Table 2. Re was compared with Re_c, which was assumed to be 10 according to Bear (1972). Subsequently, the appropriate Darcy (i.e., laminar) or non-Darcy (i.e., turbulent) flow expression (equations (9) and (10)) was selected. Non-Darcy flow regimes are identified by arrows in Figure 3.

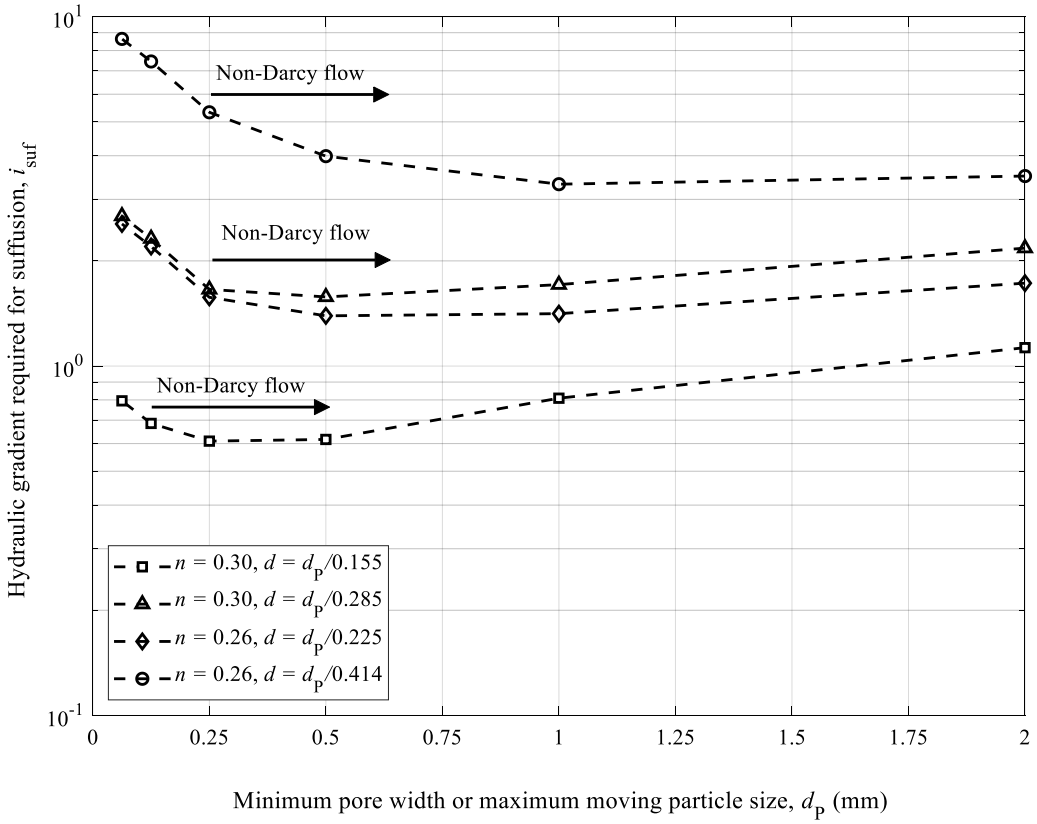

364

365 **Figure 3.** Hydraulic gradient required for suffusion (i_{suf}) for different pore widths (or
366 maximum moving particle size), d_P, and packing arrangements: double-staggered (n = 0.3)
367 with $d_P = 0.155d$ (-□-) and $d_P = 0.285d$ (-△-); pyramidal/tetrahedral (n = 0.26) with d_P =
368 $0.225d$ (-◊-) and $d_P = 0.414d$ (-o-). Arrows indicate non-Darcy flow regimes.

369

370 Kovacs (1981) suggests that the critical velocity to move a particle in a narrow tube is less than
371 half the settling velocity of isolated particles unaffected by the conduit wall and collision with
372 other particles. A large number of experiments have demonstrated that the particle settling
373 velocity is reduced in higher suspended sediment concentrations (e.g., Baldock et al., 2004) by
374 a factor usually given by the widely used semi-empirical Richardson and Zaki (1954) equation:

375 $$V_S = n^m V_T = (1-\phi)^m V_T \quad (11)$$

376

where V_S is the hindered settling velocity at porosity n, ϕ is the volumetric concentration of suspended sediments and m is an empirical exponent that ranges from 2.4 to 4.65 depending on *Re* for particles (Baldock et al., 2004).

If V_T is consequently reduced to V_S by a factor of $(1 - \phi)^m$, the value of i_{suf} (e.g., Figure 3) reduces by a similar order (for laminar flow situations). For turbulent flow, the relationship between V_T and i_{suf} is nonlinear and the effect on i_{suf} of empirical or experimentally based modification to V_T (e.g., equation (11)) requires application of non-Darcy flow theory (e.g., equations (9) and (10)).

2.3 Vertical sediment transport following fluidization of non-cohesive soils

Vertical sediment transport through preferential pathways in porous media may occur in several ways, as illustrated in Figure 1. Sediment fluidization is an important phenomenon in all cases, even where sediment rises through preferential pathways within overlying cohesive (e.g., clay, peat, etc.) layers. Fluidization is the loss of effective stress (i.e., the stress that is resisted by the soil skeleton) of non-cohesive soils, and may lead to the widely known condition of *quicksand*. It occurs when hydraulic forces accompanying flowing groundwater are sufficiently high to balance the total stress and reduce the effective stress to zero. This gives rise to a critical hydraulic gradient (i_c) at which fluidization may occur (Kovacs, 1981; Knappett and Craig, 2012). According to Terzaghi's (1922) theory:

$$i_c = \frac{\gamma_s - \gamma_f}{\gamma_f} = \frac{\gamma'}{\gamma_f} \tag{12}$$

400 Here, γ_f is the unit weight of the fluid, γ_s and γ' are the saturated and buoyant (or effective) unit
401 weight of the soil, respectively. We consider equation (12) in more detail in the following sub-
402 sections.
403
404 While the initiation of fluidization has been well studied, the mechanisms that lead to any
405 accompanying subsurface sediment transport are not well defined. Our review has encountered
406 two types of subsurface sediment transport that may arise following fluidization, which we
407 differentiate using the terms sand boils and boiling sand. Conceptual models are shown in
408 Figure 1, which illustrates two sub-categories of sand boils, including: (1) heave and
409 preferential flow through cohesive soil layers overlying non-cohesive sediments (Figure $1b_1$),
410 and (2) individual boil vents within non-cohesive soil, caused by localised discharge from
411 below (e.g., due to a fault or fracture; Figure $1b_2$). The sediment surface appears as a boiling
412 fluid where fluidization leads to more distributed sediment movement in the case of boiling
413 sand (Figure $1b_3$).
414
415 **2.3.1 Creation of preferential pathways: Heave and pipe formation**
416
417 The hydraulic gradient required to cause heave in both cohesive and non-cohesive sediments,
418 and sand boils and boiling sand in non-cohesive sediments is, theoretically at least, Terzaghi's
419 (1922) i_c (i.e., equation (12)) (Kovacs, 1981; Wan and Fell, 2004; Knappett and Craig, 2012;
420 FEMA, 2015). In cohesive soils, heaving can create concentrated outflows of seepage to the
421 land surface through weaknesses (e.g., through hydraulic fracturing) in upper soil layers, in the
422 form of holes or cracks (Figure $1b_1$) (e.g., Mansur et al., 2000; Glynn and Kuszmaul, 2010; van
423 Beek et al., 2011). This may result in localised discharge, which de Louw et al. (2010, 2013)
424 referred to as 'sand boils' or simply 'boils' depending respectively on whether or not sediment

425 is ejected. FEMA (2015) describe two alternative approaches to the estimation of heave, based
426 on whether force balances are undertaken using the effective stress or the total stress. In both
427 cases, heave is predicted to occur when the hydraulic gradient equals Terzaghi's (1922) i_c.
428 However, preferential pathways may arise in cohesive layers at hydraulic gradients well below
429 i_c due to hydraulic fracturing (FEMA, 2015). Petrula et al. (2019) conducted extensive
430 laboratory experiments on glass beads subjected to upward seepage flow and compared the
431 measured critical hydraulic gradients for heave to calculated i_c using three different formulae
432 developed during 1922-1931, and found that the Terzaghi's (1922) formula (i.e., equation (12))
433 provides the best prediction of i_c.
434
435 As discussed above and illustrated in Figure 1, two types of conduit flow are apparent in
436 previous studies of non-cohesive soils: sand boils (point discharge) and boiling sand (dispersed
437 discharge). Differentiating between the mechanisms that create sand boils versus boiling sand
438 requires some speculation, because the distinction has not been investigated previously.
439 Perhaps the former, sand boils, are found where conduits in non-cohesive soil bodies originate
440 from a source of localised discharge (e.g., through a fault or fracture) below the non-cohesive
441 soil body, as illustrated in Figure $1b_2$. Where upward seepage is dispersed (rather than
442 localised) and sufficiently high to disturb the non-cohesive sediment structure over an area
443 (rather than localised points causing discrete sand boils), this may lead to multiple pathways of
444 instability in the soil structure, creating recirculation of particles in the form of boiling sand
445 (Figure $1b_3$). In any case, the occurrence of both sand boils and boiling sand in non-cohesive
446 soils requires the creation of preferential pathways (Wan and Fell, 2004). Discharge must be
447 high enough to carry sand grains to the land surface and to maintain preferential flow conduits
448 within the non-cohesive sediment body. In the case of boiling sand, it is likely that those
449 pathways are continuously changing. Wan and Fell (2004) state that the hydraulic gradient

leading to boiling sand is again theoretically equal to Terzaghi's (1922) i_c. However, their experimental results for silt-sand-gravel and clay-sand-gravel soil mixtures showed that hydraulic gradients greater than i_c were needed for sand boils or boiling sand to occur. They attributed this to inter-particle electrochemical forces in soil mixtures containing silt or clay.

2.3.2 Flow through preferential pathways

For simplicity, conduits in both non-cohesive and cohesive soils are often treated as pipes, through which water is assumed to flow at high rates relative to flow through the surrounding sand matrix. The preferential pathways associated with sand boils (in both cohesive and non-cohesive sediment; Figure 1b$_1$ and 1b$_2$) are approximated in the analysis that follows as vertical pipes, allowing use of the Darcy-Weisbach formula to describe their flow, as (Bear, 1972):

$$i_P = f \frac{1}{D_P} \frac{V_P^2}{2g} \tag{13}$$

where i_P is the hydraulic gradient in the pipe, f is the friction factor, D_P is the pipe diameter, and V_P is the flow velocity in the pipe. Re for pipe flow is obtained from equation (2), with $L = D_P$ and $U = V_P$. When $Re \leq 2320$, laminar pipe flow can be assumed in the preferential pathway (van Beek et al., 2013), and the Hagen-Poiseuille formula (Hagen, 1839; Poiseuille, 1841) can be used by adopting $f = 64/Re$ in equation (13). When $Re > 4000$, turbulent pipe flow occurs, and f is a function of Re and the relative roughness, ε/D_P, where ε is the roughness of the pipe wall and is a function of grain size distribution, grain shape and grain spacing (e.g., Kamphuis, 1974). Various expressions and methods are available to find f for turbulent flow, including the Colebrook equation, given as (Nakayama, 1999):

$$\frac{1}{f} = -2\log\left(\frac{\varepsilon/D_P}{3.71} + \frac{2.51}{Re\sqrt{f}}\right) \tag{14}$$

The above theory allows for estimates of i_P required to produce V_P values that coincide with Table 2 values of V_T, i.e., hydraulic gradients needed to bring sediments of various sizes to the surface through vertical pipes. Values of d and D_P ranging from 0.0625 mm to 2 mm (as per Table 2 diameters) were evaluated for cases where $d \leq D_P$, i.e., particles theoretically able to pass through the pipe. Calculated values of Re ($0.2 \leq Re \leq 560$) indicated that in all cases, laminar flow conditions are expected. Values of i_P arising from these calculations are shown in Figure 4.

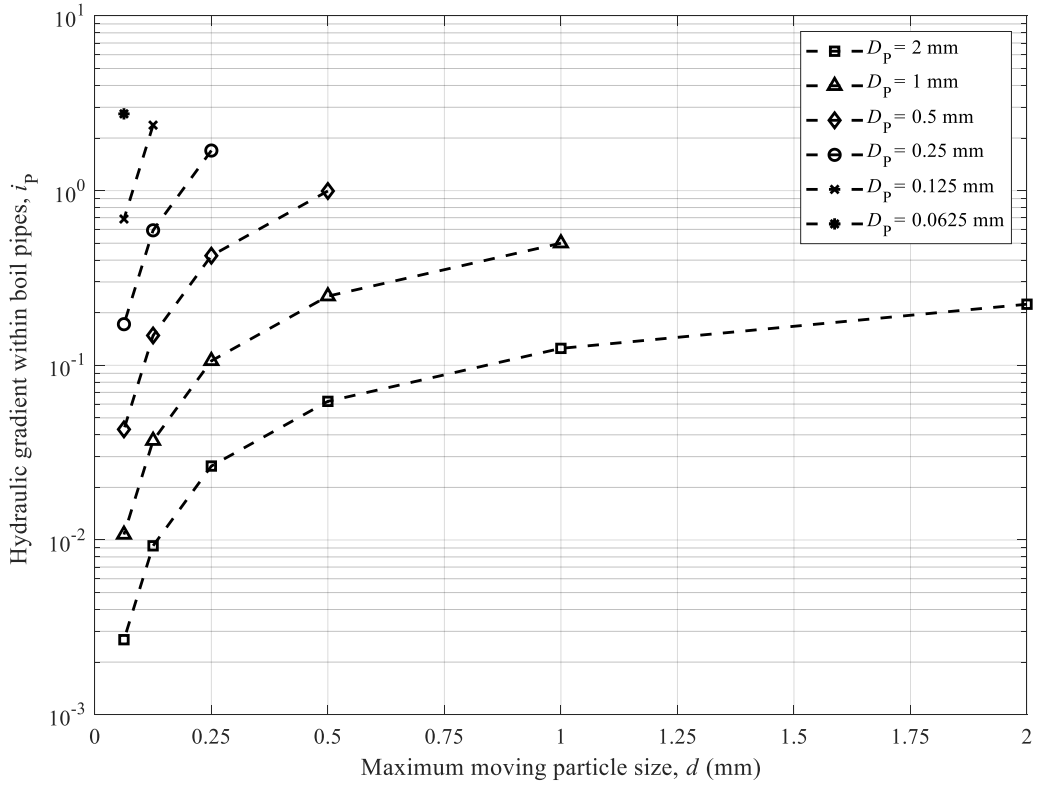

Figure 4. Hydraulic gradients within boil 'pipes' (i_P) for different moving particle sizes (d) and pipe diameters (D_P).

2.4 Subsurface flow processes: Hypothetical modelling of conceptual models

In the previous sub-sections, estimates are provided of hydraulic gradients required to cause heave and to move particles through immobile porous matrices and through preferential pathways. The conceptual models adopted in developing the above theory involve various combinations of non-cohesive materials (e.g., sand), with and without preferential flow paths (e.g., flow pipes), and with and without overlying/underlying cohesive layers (e.g., overlying clay or underlaying faulted bedrock). The subsurface head distributions (and corresponding flow directions) accompanying these conceptual models are rarely considered in previous studies. Therefore, to assist in the understanding of subsurface flow processes associated with the previous situations, several hypothetical scenarios of simplified aquifer cross-sections are devised and modelled. Steady-state groundwater flow was simulated using MODFLOW (Harbaugh, 2005) to demonstrate the effects of preferential flow and layering on subsurface flow conditions. We neglect pipe flow and treat preferential flow features as equivalent porous medium, amongst other simplifying assumptions that allow for conceptual demonstration of subsurface flow in uncomplicated scenarios.

The conceptual models are illustrated in Figure 5, which also provides the head distributions arising from MODFLOW simulations. Flow is considered in cross-sections of 10 m depth by 10 m horizontal length (N.B., scale distortion of approximately 1:4 is used in Figure 5). Flow directions are perpendicular to head contours. The boundary conditions in all cases are specified head conditions at the top (hydraulic head = land surface) and bottom (hydraulic head = 10 m above land surface), creating a hydraulic gradient of 1.0 that is uniform throughout the subsurface in the absence of aquifer heterogeneity (see Figure 5a). No-flow conditions apply to the side boundaries, and other parameters are shown in Figure 5.

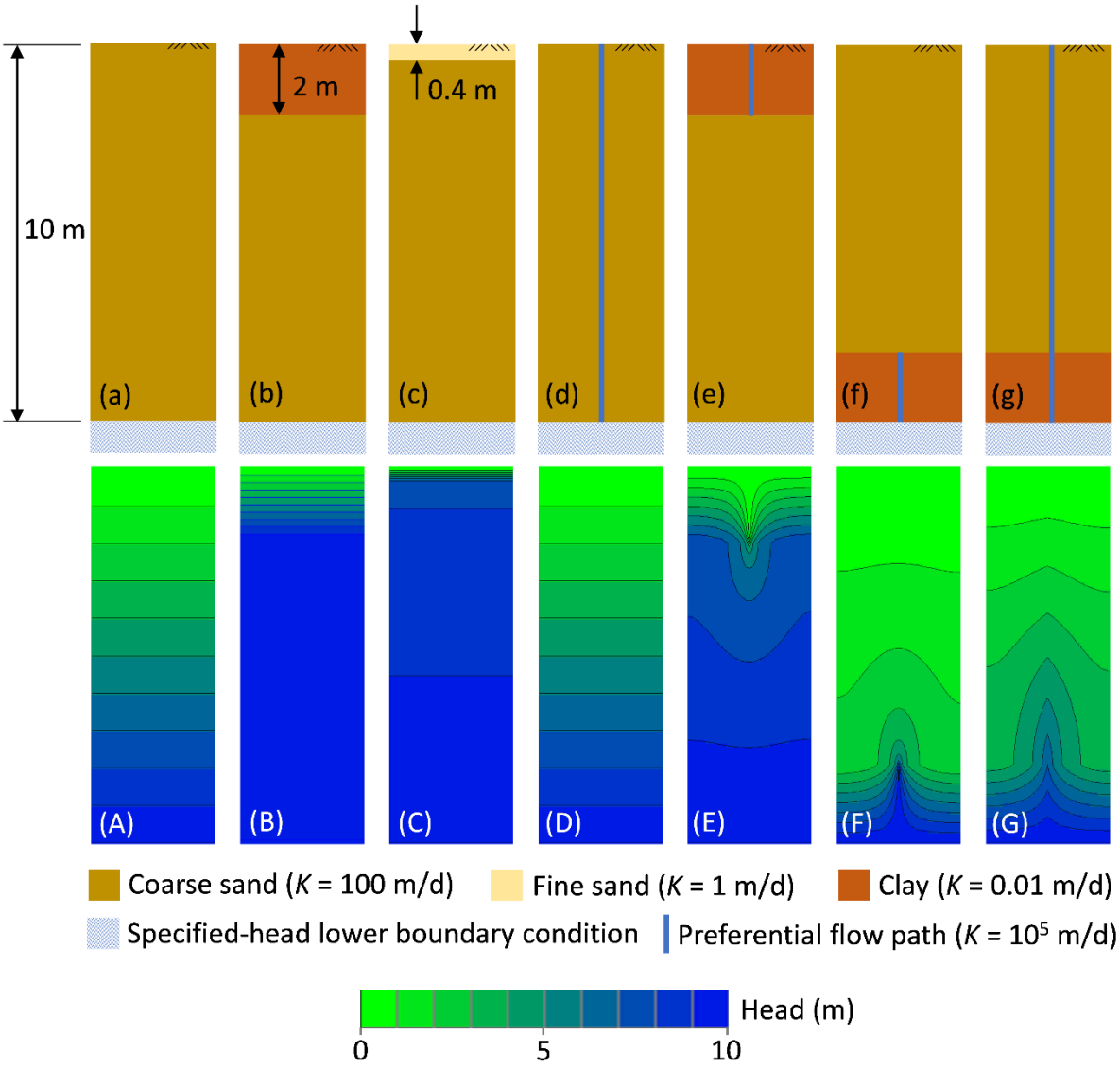

513

514 **Figure 5.** Hypothetical conceptual models (a) to (g) and corresponding head distributions (A)
515 to (G) showing various situations of vertical flow. These include: (a) homogeneous coarse
516 sand; (b) clay overlying coarse sand; (c) fine sand overlying coarse sand; (d) homogeneous
517 coarse sand with a fully penetrating preferential flow feature; (e) clay, containing a
518 preferential flow feature, overlying coarse sand; (f) coarse sand overlying clay containing a
519 preferential flow feature; (g) coarse sand overlying clay with a fully penetrating preferential
520 flow feature.

521

The results shown in Figure 5 highlight important subsurface flow processes of relevance to the conceptual models of earlier sub-sections. For example, relatively high hydraulic gradients occur in low-*K* layers that overly high-*K* layers (Figures 5B and 5C). For the simple configuration of Figure 5, manipulation of Darcy's Law shows that:

$$\frac{i_{\mathrm{U}}}{i_{\mathrm{L}}} = \frac{K_{\mathrm{L}}}{K_{\mathrm{U}}} \tag{15}$$

$$i_{\mathrm{U}} = \frac{\Delta h}{\frac{K_{\mathrm{U}}}{K_{\mathrm{L}}} L_{\mathrm{L}} - L_{\mathrm{U}}} \tag{16}$$

where subscripts L and U refer to lower and upper layers, *i* is hydraulic gradient, *K* is isotropic hydraulic conductivity, and Δh is the head drop (10 m in Figure 5) across the subsurface profile. Equation (16) allows for rapid assessment of gradients in low-*K* surface layers (for initial estimation of the potential for heave). Note that i_{U} is higher in the fine sand case (i.e., Figure 5C; $|i_{\mathrm{U}}| = 32.9$) than in the clay case (i.e., Figure 5B; $|i_{\mathrm{U}}| = 1.25$). It follows that where relatively fine materials are deposited over coarse sediment in groundwater upwelling zones, these are highly susceptible to fluidisation because they are likely to experience significant hydraulic gradients relative to the situation before deposition.

The addition of a fully penetrating, vertical, preferential flow feature to the homogeneous case (i.e., Figure 5d) does not modify the flow field in the coarse sand (Figure 5D). Thus, it follows that development of fully penetrating preferential flow features may not reduce the potential for fluidization elsewhere in non-cohesive sediments, because the same hydraulic gradients may occur in the parent material both with and without vertical preferential pathway (Figures 5A and 5D). Hence, under idealistic homogeneous conditions, pipes may develop in sand

544 bodies without necessarily reducing the likelihood of other pipes forming, given stable
545 boundary conditions below the sand.
546
547 Figure 5e represents a situation where the overlying low-*K* layer contains a preferential flow
548 path, as might occur following heave (see Section 2.3.1). A comparison of head contours with
549 and without the preferential pathway (Figures 5E and 5B) shows that it creates considerably
550 higher flow in the coarse sand (i.e., larger i_L; more closely spaced head contours), and
551 significantly reduces i_U (i.e., more sparsely spaced head contours). Thus, the development of
552 preferential pathways in low-*K* surface layers reduces the likelihood of heave and additional
553 preferential pathways forming within the low-*K* layer in the near vicinity.
554
555 Figure 5f illustrates the situation of a high-*K* feature within an otherwise low-*K* layer,
556 underlying a coarse sand body, consistent with the conceptual model of Figure $1b_2$, except no
557 preferential flow features are simulated within the coarse sand. The MODFLOW results show
558 a high hydraulic gradient (approximately equal to 19 in the vertical direction) at the base of the
559 coarse sand layer where the preferential flow feature terminates. This supports the conceptual
560 model of Figure $1b_2$, whereby fluidization may be induced locally around such features. Figure
561 5g builds on the situation of Figure 5f by extending the preferential flow feature through the
562 coarse sand layers to the land surface. Whereas the steep head gradients at the base of the coarse
563 sand layer dissipate over short distances in Figure 5f, the preferential flow feature in the coarse
564 sand in Figure 5g reduces head gradients at the base of the coarse sand, and increases gradients
565 in the middle and upper sections. It follows that preferential flow features that develop within
566 sand bodies, under conditions similar to Figure 5g, propagate the high hydraulic gradients
567 needed for fluidization over larger vertical extents than otherwise occurs without preferential

568 flow paths. In other words, preferential flow paths tend to maintain and propagate the head
569 gradients required for their occurrence (i.e., fluidization).
570
571 **3. Experimental studies**
572
573 The results of suffusion, fluidization and sand boil experiments are critical for assessing theory
574 of the type described above, given the many simplifying assumptions adopted in the respective
575 force equilibrium methods. The theory presented above does not account for friction arising
576 from the collision of moving particles or between moving particles and the stationary porous
577 matrix, or other factors including electrochemical forces and other phenomena that modify the
578 capacity for particles to move due to hydraulic forces.
579
580 **3.1 Suffusion experimental studies**
581
582 The initiation of piping, erosion processes and fine particle displacement rates caused by
583 suffusion has been observed in laboratory experiments predominantly aimed at studying the
584 onset and mechanisms of piping failure (e.g., de Wit et al., 1981; van Beek et al., 2011). For
585 example, Sterpi (2003) used laboratory experiments of erosion and transport of fine particles
586 in a silty sand subjected to an upwards vertical seepage flow to produce an empirical equation
587 relating particle transport to the experimental parameters. The experimental results showed that
588 the percentage of eroded fine particles increased with time under a constant hydraulic gradient,
589 and also increased with hydraulic gradient for constant periods of time.
590
591 Liang et al. (2017) designed a stress-controlled apparatus to investigate particle erosion under
592 different stress states (i.e., combinations of vertical and confining stresses) and upwards

593 seepage flow rate, by using a soil-water separating system. The results of their study showed
594 that a specimen would collapse when the amount of eroded fine particles exceeded a critical
595 proportion of the soil weight.
596
597 Wan and Fell (2004) investigated the internal stability of soils (mixtures of sand, gravel, silt,
598 and clay) with respect to their susceptibility to suffusion by conducting both upward flow and
599 downward flow seepage tests. The hydraulic gradient at which suffusion was initiated was
600 recorded. They defined a hydraulic gradient, i_{start}, at which the first sign of erosion of fine
601 particles (e.g., observation of cloudiness in the flow) was observed. Wan and Fell's (2004)
602 laboratory results showed that suffusion started at lower hydraulic gradients than that predicted
603 by equation (12), i.e., i_{start} < Terzaghi's (1922) i_c for all unstable and many stable soil samples.
604 Wan and Fell (2004) observed an inverse relationship between n and i_{start}, whereby soils with
605 higher n would be eroded at lower upward gradients. In other words, a higher i_{start} was required
606 to erode a soil with higher γ_s. The theory of Kovacs (1981) is consistent with this general
607 relationship. The same trend is generally applicable to the functions given in Figure 3, in that
608 the lowest and highest values of i_{suf} arose from the higher (0.3) and lower (0.26) n values,
609 respectively. Wan and Fell's (2004) laboratory experiments also showed the effect of
610 cohesiveness between particles, in that i_{start} was higher for soils with higher clay contents.
611
612 Ahlinhan and Achmus (2010) conducted several laboratory experiments on stable and unstable
613 non-cohesive soils under upward and horizontal seepage flows to study the i_{start}. They
614 determined the i_{start} where significant change (i.e., a strong increase) was observed in flow
615 velocity and the mass of eroded fine particles. Their experiments showed that for unstable soils,
616 the critical hydraulic gradient for upward flow slightly depends on the relative density (D_r),
617 which is an indicator of the degree of compaction in non-cohesive soils and is expressed as D_r

618 = $(e_{max}-e)/(e_{max}-e_{min})\times100\%$ where e is the void ratio of soil in natural state, e_{max} and e_{min} are
619 the maximum and minimum limits of e corresponding to the loosest and densest states of soil
620 respectively, while a distinct dependence of critical hydraulic gradients on D_r was found for
621 stable soils.
622
623 In laboratory experiments on sandy soils under upward flow, Fleshman and Rice (2014)
624 observed that i_{start} was higher than both Terzaghi's (1922) i_c and values reported in previous
625 laboratory research (e.g., Skempton and Brogan, 1994). This contradicts Wan and Fell's (2004)
626 earlier results. Fleshman (2012) attributed these differences to the respective laboratory
627 methodologies, in that in previous experiments, hydraulic gradients were measured across
628 entire soil samples whereas the measurements of Fleshman and Rice (2014) focused on
629 hydraulic gradients across smaller scales, namely at the seepage exit point. However,
630 Schmertmann (2015) argued that the higher hydraulic gradient measured by Fleshman and Rice
631 (2014) are seriously inconsistent with previous theory and laboratory and field experiments
632 because of high friction between the interface of sample holder and the soil sample (i.e., sample
633 side shear), the obstruction of the pore pressure probes to water and particle movement and
634 resulting arching effects; hence, the Fleshman and Rice's (2014) results have not been used in
635 the current study.
636
637 In the following, the theory developed in Section 2.2 for suffusion is compared to the
638 experimental results of Wan and Fell (2004) and Ahlinhan and Achmus (2010). While i_{start}
639 likely applies to the smallest particles within a soil, i_{suf} applies to the largest potentially mobile
640 particles, and thus $i_{start} < i_{suf}$ is expected, at least theoretically. Soil and experimental properties
641 and the results of upward flow seepage tests by Wan and Fell (2004) and Ahlinhan and Achmus
642 (2010) are given in Table 5. Wan and Fell (2004) observed three stages in their experiments

643 and measured the hydraulic gradient in each stage, including (1) initial loss of fine particles,
644 (2) extreme cloudiness, and (3) boiling sand development. The *i* values of Ahlinhan and
645 Achmus (2010) in Table 5 correspond to the erosion of fine particles where a strong increase
646 in mass transport and flow velocity was measured in their experiments, although Ahlinhan and
647 Achmus (2010) observed some grain movements on the sample surface at smaller hydraulic
648 gradients than those in Table 5.
649

650 **Table 5.** Summary of soil properties and upward flow seepage test results of Wan and Fell
651 (2004) and Ahlinhan and Achmus (2010).

Test no.	Particle density, ρ_s (kg/m^3)	d_{10} (mm)	d_{15} (mm)	d_{50} (mm)	Porosity, n	Hydraulic gradient, i			Reference
						Initial loss of fines	Extreme cloudiness	Boiling	
1	2620	0.057	0.085	4.750	0.169	2.20	2.54	2.32	Wan and Fell (2004)
					0.210	0.78	1.17	1.95	
2R	2620	0.028	0.051	3.68	0.214	0.99	1.38	2.93	
3R	2610	0.012	0.018	0.137	0.292	0.73	1.12	N/O	
4R	2600	0.258	0.425	4.750	0.191	0.80	2.19	3.58	
5	2570	0.082	0.252	3.180	0.218	3.17	3.77	3.97	
					0.261	0.18	N/O	1.54	
9	2680	0.066	2.340	6.550	0.315	0.14	N/O	N/O	
10	2690	0.022	0.037	5.650	0.217	0.59	0.78	2.52	
					0.256	0.37	0.94	1.12	
11	2670	0.011	0.011	0.120	0.319	0.76	0.68	0.88	
14A	2680	0.007	0.016	7.110	0.270	0.77	N/O	3.92	
					0.315	0.17	0.56	1.33	
15	2570	0.001	0.006	6.030	0.228	0.80	N/O	3.18	
A1	2650	0.094	0.104	0.172	0.495	0.70	–	–	Ahlinhan and Achmus (2010)
					0.467	0.80	–	–	
					0.435	0.90	–	–	
					0.412	0.95	–	–	
A2	2650	0.210	0.254	0.526	0.380	0.90	–	–	
					0.351	0.96	–	–	
					0.330	0.97	–	–	
E1	2650	0.210	0.558	1.321	0.383	0.30	–	–	
					0.375	0.36	–	–	
					0.353	0.60	–	–	
E2	2650	0.109	0.362	1.233	0.353	0.19	–	–	
					0.341	0.21	–	–	
					0.293	0.25	–	–	
E3	2650	0.109	1.061	2.231	0.341	0.19	–	–	
					0.316	0.21	–	–	

652 N/O – Not observed

653
654 Figure 6 compares theoretical hydraulic gradients needed for suffusion (i_{suf}) based on the theory
655 presented here with experimental values (i_{exp}) of Wan and Fell (2004) and Ahlinhan and
656 Achmus (2010). Values of i_{exp} were taken as those required for the initial loss of fines (Wan
657 and Fell, 2004; Ahlinhan and Achmus, 2010; Table 5). To calculate i_{suf}, several assumptions
658 were required, including (1) the soil particles are spherical in shape and soil properties (i.e., ρ_s,
659 d_{10}, d_{15}, d_{50}, and n) are given in Table 5, (2) the water properties are constant i.e., $\rho_f = 10^3$

660 kg/m^3, and μ = 10^{-3} Pa.s, (3) d_P is proportional to d_{50}, with proportionality based on the four
661 different packing arrangements of Table 3 (i.e., double-staggered and pyramidal/tetrahedral,
662 with two alternative values of d_P for each arrangement), (4) the maximum size of moving
663 particles is equal to d_P, (5) equation (7) is used to calculate V_T where $d = d_P$, (6) k is obtained
664 from equation (8) where c_0 = 1/2 and $d = d_{50}$, (7) Re is calculated by equation (2) where L =
665 d_{10}, $U = q = nV_G$, and $V_G = V_T$, (8) Re_c is 10, and (9) equations (9) and (10) are used to calculate
666 i_{suf}. Assumption (1) is expected to overpredict i_{suf}, because V_T tends to be lower for natural
667 particles relative to spheres (e.g., Arora et al., 2009). Assumptions (4) and (5) are also expected
668 to overpredict i_{suf}, because suffused particles are likely to be smaller than d_P. An alternate value
669 of c_0 (e.g., Fitts (2002) adopts c_0 equal to 1/5) would lead to lower k values for a given d, and
670 therefore assumption (6) tends to underpredict i_{suf}.

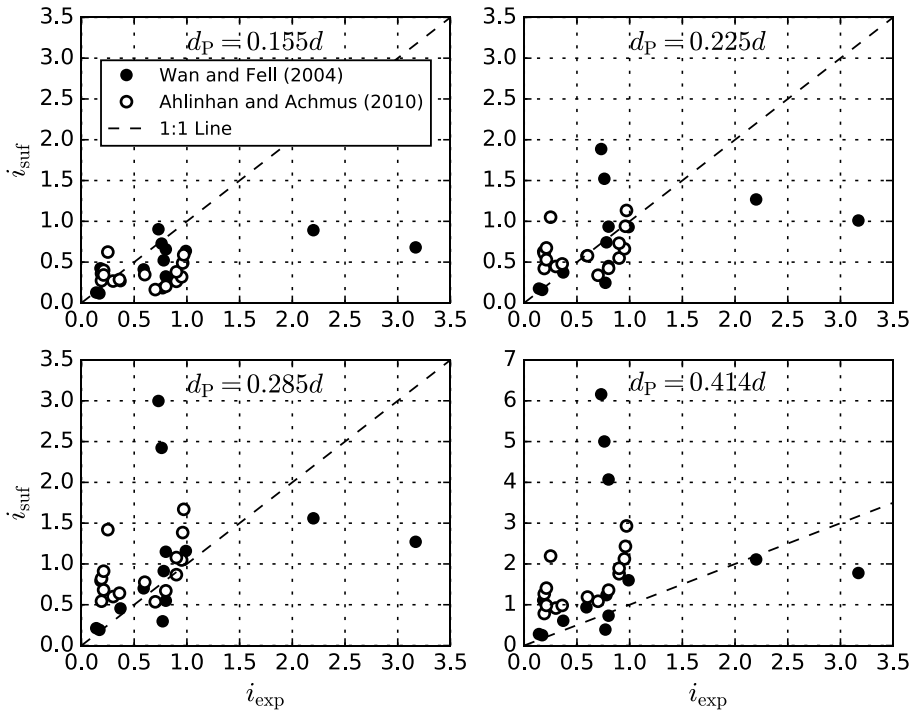

671

672 **Figure 6.** Comparison between i_{suf} (suffusion theory described in earlier sections) and i_{exp}
673 from the suffusion experiments of Wan and Fell (2004) and Ahlinhan and Achmus (2010).

The four sub-figures show alternative assumptions (see Table 3) regarding the relationship between minimum pore size (d_P) and sediment diameter (d).

The Figure 6 results show relationships between i_{suf} and i_{exp} that vary from $i_{suf} > i_{exp}$ (e.g., generally the case where $d_P = 0.414d$) to $i_{suf} < i_{exp}$ (e.g., generally the case in $d_P = 0.155d$), although in all cases there is scatter across the 1:1 line. The comparisons show approximate correlation between theory and experimental results except for the highest i_{exp} value, which is underpredicted by i_{suf} in all four of the packing arrangements of Figure 6. For the largest values of i_{suf} (e.g., where $d_P = 0.414d$), i_{suf} exceeds significantly i_{exp}, although where $d_P = 0.155d$, the match is improved. The larger deviations between i_{exp} and i_{suf} at higher hydraulic gradients may be related to the transition of flow from laminar to turbulent, which is not considered in the calculation of i_{suf} using equation (9). That is, in equation (9), the flow regime within the porous media is divided into laminar or turbulent based on *Re* values, whereas the occurrence of laminar/turbulent flow in the transient, preferential flow processes leading to the onset of boils is not taken into account. Statistical criteria including mean absolute error (MAE), root mean square error (RMSE), percent bias (PBIAS) and Nash-Sutcliffe efficiency (NSE) (Moriasi al., 2007) are presented in Table 6 to evaluate the match between i_{suf} and i_{exp}. MAE, RMSE, PBIAS values closer to 0 and NSE closer to 1 indicate better agreement (Moriasi al., 2007). Accordingly, packing arrangements with $d_P = 0.225d$ shows better match between i_{suf} and i_{exp}.

Table 6. Statistical criteria to evaluate i_{suf} and i_{exp} comparison for suffusion.

	$d_P = 0.155d$	$d_P = 0.285d$	$d_P = 0.225d$	$d_P = 0.414d$
MAE	0.396	0.502	0.375	1.120
RMSE	0.622	0.751	0.582	1.660
PBIAS (%)	41.88	-35.25	2.252	-136.7
NSE	0.001	-0.456	0.125	-6.119

3.2 Sand boil experimental studies

Townsend et al. (1988) and Schmertmann (2000) obtained minimum gradients for piping in the lateral direction in clean, fine, uniform sands. Based on their laboratory tests, this type of sand was found to experience backward erosion piping at gradients as low as 0.08, although this appears model a severe scenario in that a highly erodible soil was used and a roof consisting of a plexiglass plate was placed above it. The low gradients for piping in Townsend et al. (1988) and Schmertmann (2000) experiments also attributed to local concentrations of flow lines at the entrance and discharge areas of the seepage flow and after pipe formation, near the pipe tip. The vertical movement of particles, which is the focus of the current review, differs to lateral particle movement, in which the stabilizing force includes the friction that inhibits particle rotation (e.g., along the horizontal plane), as opposed to the requirement for the effective stress to drop to zero in vertical sand transport situations (Worman and Olafsdottir, 1992). Thus, vertical sediment movement likely requires higher hydraulic gradients relative to lateral sediment movement.

Studies that reveal rates of vertical sediment transport through sand boils are uncommon relative to piping and suffusion experiments, and investigations that obtain i_c. Fujisawa et al. (2013) investigated the relationship between seepage forces and sand particle velocities due to upward and horizontal seepage flows within a vertical U-shaped cylinder and a horizontal pipe, respectively, in laboratory experiments. Sand particle velocities obtained in their experiments were well estimated by force equilibrium analysis similar to that described herein (i.e., comparison of seepage, buoyancy and gravity forces).

Laboratory experiments evaluating i_c in sandy gravels subjected to upward flow were conducted by Skempton and Brogan (1994), who found that piping occurred at i_c values similar

to Terzaghi's (1922) i_c when soils were internally stable. Otherwise, piping occurred at lower values of i_c (i.e., one-third to one-fifth of Terzaghi's (1922) i_c) when the samples were internally unstable. Skempton and Brogan (1994) explained the discrepancy between experimental i_c and Terzaghi's (1922) i_c for internally unstable soil by that the greater part of the overburden load is carried by coarser particles, leaving most of the finer particles under small pressure, i.e., a reduction in γ' in equation (12). Similar findings were obtained by Yang and Wang (2017), who undertook laboratory experiments on uniform sand (considered internally stable) and gap-graded sand (considered internally unstable). They compared 44 measured i_c values with i_c predictions from four alternative models, all based on the force equilibrium of a single soil particle. Comparison of predicted and measured i_c values showed that no single predictive model was applicable to all soil types.

Comprehensive studies aimed at controlling seepage and sand boils along the lower Mississippi River levees (e.g., Turnbull and Mansur 1959; USACE, 1956) showed that the upward gradient required to cause sand boils varied from 0.5 to 0.8 at different sites. The gradient was determined by measuring the hydrostatic head beneath the top stratum (blanket) at the time sand boils first appeared (i.e., $i_c = h_{blanket}/z_{blanket}$, where $h_{blanket}$ is the head beneath the blanket and z is the thickness of the blanket). Accordingly, USACE (2005) recommends $i_c = 0.5$ as the minimum gradient required to cause sand boils. In The Netherlands, TACFD (1999) assumed $i_c = 0.3$ based on fluidisation experiments of Yap (1981). A comparison between US and Dutch criteria for sand boils and piping can be found in Ammerlaan (2007).

In the sand boil, the head loss is not constant vertically through the sand boil and it is a function of sand properties, the size of sand boil and the flow rate (Robbins et al., 2019). Some recent studies (e.g., Bezuijen, 2015; Bezuijen et al., 2019; Robbins et al., 2019) have developed

747 theoretical models to examine the head loss in a sand boil based on settling velocities in a
748 vertical pipe that are hindered by suspended sediments. Robbins et al. (2019) compared their
749 theory with head loss measurements in boils along the Mississippi River in the USA and the
750 Waal River in The Netherlands, and also Yap's (1981) experiments. They found reasonably
751 good agreement between measurements and their theory.
752
753 Theoretical and laboratory values for the hydraulic gradient required to create sand boils are
754 compared in Figure 7, in which i_c is based on the theory developed in Section 2.3 in the case
755 of sediment transport following fluidization of non-cohesive soils (sand boils) and i_{exp}
756 observations are taken from the studies of Wan and Fell (2004) (Table 5; *i* value at which
757 "extreme cloudiness" was observed, as a possible indication of the onset of sand boil
758 formation), Skempton and Brogan (1994) and Yang and Wang (2017) (Table 7). It should be
759 noted that images of Skempton and Brogan (1994) and Yang and Wang (2017) experiments
760 identify individual sand boils and therefore we consider that their results are applicable to the
761 theory developed in Section 2.3.
762
763 **Table 7.** Summary of soil properties and upward flow seepage test results of Skempton and
764 Brogan (1994) and Yang and Wang (2017).

Test no.	Particle density, ρ_s (kg/m^3)	d_{10} (mm)	d_{15} (mm)	d_{50} (mm)	Porosity, n	Hydraulic gradient, i_{exp}	Reference
S1	2650	0.089	0.095	0.149	0.490	0.69	Skempton and Brogan (1994)
S2	2650	0.220	0.259	0.501	0.460	0.90	
S3	2650	0.106	0.123	0.233	0.380	1.01	
F	2650	0.716	0.745	0.801	0.400	1.05	
A	2650	0.181	0.600	3.854	0.340	0.20	
AF	2650	0.181	0.600	3.854	0.340	0.18	
B	2650	0485	0.900	3.854	0.370	0.34	
C	2650	0.662	0.980	3.854	0.375	1.00	
D	2650	1.080	1.600	4.137	0.365	1.00	
B	2650	0.175	0.189	0.280	0.420	0.89	Yang and Wang (2017)
C	2650	0.708	0.806	1.170	0.410	0.86	
G	2650	0.298	0.407	3.710	0.400	0.57	

The assumptions used in calculating i_c are: (1) fine particles transport through vertical preferential pathways, (2) Tables 5 and 7 provide soil properties (i.e., ρ_s, d_{10}, d_{15}, d_{50}, and n) and soil particles are spherical in shape, (3) the water properties are constant i.e., $\rho_f = 10^3$ kg/m^3, and $\mu = 10^{-3}$ Pa.s, (4) the maximum size of moving particles is equal to d_{10}, (5) the vertical preferential pathway has a circular cross-section (pipe) and the diameter of the pipe (D_P) should be bigger than the maximum size of moving particles (i.e., d_{10}), here assumed $D_P = d_{15}$. In other words, d_{15} is the initial pipe size at the start of sand boil allowing to particles with d_{10} pass through, (6) equation (7) is used to calculate V_T where $d = d_{10}$, (7) Re is calculated by equation (2) where $L = D_P$, $U = V_P$, and $V_P = V_T$, and (8) equation (13) is used to calculate i_c where $f = 64/Re$ ($Re < 2320$ indicating laminar pipe flow).

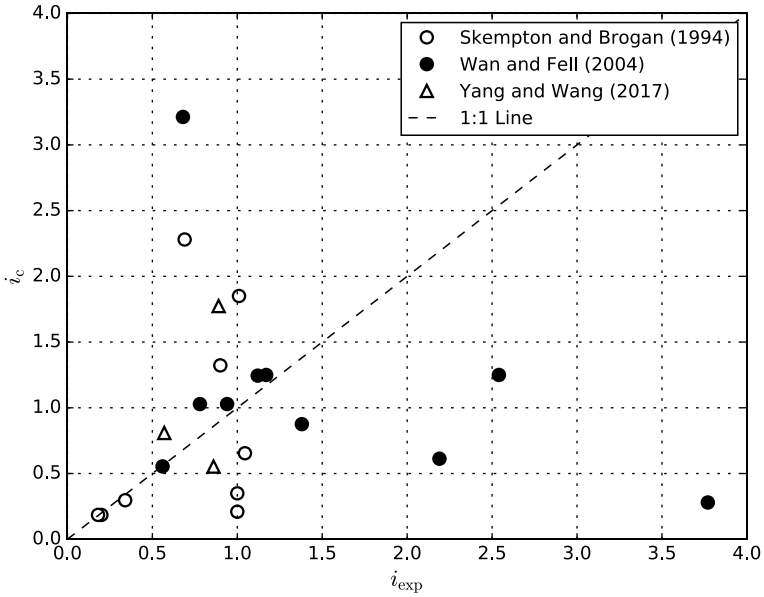

Figure 7. Comparison between hydraulic gradients required to form sand boils using the theory of Section 2.3 (i_c) and the experiments of Skempton and Brogan (1994), Wan and Fell (2004) and Yang and Wang (2017) (i_{exp}).

781 Using d_{10} as the maximum size of moving particle and d_{15} as the minimum pipe diameter
782 (assumptions 4 and 5, respectively) provides the best agreement between theoretical (i_c) and
783 experimental (i_{exp}) hydraulic gradients required to form sand boils. Figure 7 shows that
784 approximately 32% of the experimental values (i_{exp}) are well predicted by theory with less than
785 13% difference, but otherwise, the match is poor. Clearly, the theory underpinning i_c (as
786 described above) does not account for processes that are precursors to sand boil (and boiling
787 sand) formation. This is discussed in more detail in the following section.
788
789 **4. Discussion**
790
791 Comparison can be made between the hydraulic gradients required to initiative heave (i.e.,
792 Terzaghi's (1922) i_c, although lower hydraulic gradients may create hydraulic fracturing;
793 Section 2.3.1) and those associated with suffusion (i.e., i_{suf}; Figure 3). Equation (12) is applied
794 to obtain estimates of i_c with γ_f = 9.8 kN/m^3 and noting that the two values of n in Table 3
795 equate to γ_s values of 21.14 and 21.79 kN/m^3 for n = 0.3 and 0.26, respectively (assuming ρ_s =
796 2650 kg/m^3 and ρ_f = 1000 kg/m^3). Thus, the value of Terzaghi's (1922) i_c for double-staggered
797 (n = 0.30) and pyramidal/tetrahedral (n = 0.26) packing arrangements is 1.16 and 1.22. For the
798 same values of n, i_{suf} in Figure 3 varies from around 0.6 (the lowest value on the dashed line
799 with square markers where d_P = 0.25 mm) to 8.6 (the highest value on the dashed line with
800 circle markers where d_P = 0.0625 mm). Assuming that Terzaghi's (1922) i_c causes heave (i.e.,
801 i_c equal to 1.16 and 1.22), then heave theoretically occurs at hydraulic gradients that are lower
802 than all i_{suf} values in Figure 3 (i.e., for all values of d) for the three packing arrangements that
803 produce the largest pore spaces (i.e., d_P = 0.225d to 0.414d). This seems prima facie to
804 contradict the combined experimental findings of Wan and Fell (2004), who noticed suffusion
805 prior to boiling and without reporting that any heave occurred. However, theoretical i_{suf} values

used in the current study are those that require the largest particles capable of fitting through pore spaces to mobilise, and therefore, the first signs of suffusion should occur at gradients less than theoretical i_{suf} values. In reality, suffusion likely precedes heave, given that smaller particles require lower V_T values (Table 2) and therefore lower i_{suf}. However, heave is probably the precursor to the development of sand boils where there is no pre-existing defect (e.g., crack, root hole, animal burrow) in the soil layer, because the hydraulic gradient required for initial particle movement (Figure 3) generally exceeds Terzaghi's (1922) i_c, as discussed above.

Intuitively, boiling sand probably occurs at higher hydraulic gradients relative to isolated sand boils. Notwithstanding the general concepts discussed above, the sequence of sediment transport processes accompanying high upward hydraulic gradients is likely to differ depending on specific circumstances. This is reflected in the summary of comparisons between hydraulic gradients required to initiate sand boils and boiling sand (i_c) and suffusion (i_{start}), and Terzaghi's (1922) i_c, given in Table 8.

Table 8. Summary of literature comparing critical hydraulic gradients for different forms of subsurface sediment transport based on theory and experiments.

Laboratory experiments	Results	Comments
Skempton and Brogan (1994)	i_c ~ Terzaghi's (1922) i_c	Sand boil, internally stable soils
	i_c ~ 1/3 to 1/5 Terzaghi's (1922) i_c	Sand boil, internally unstable soils
Wan and Fell (2004)	i_{start} < Terzaghi's (1922) i_c	Suffusion, for all internally unstable and many internally stable soils
	i_c > Terzaghi's (1922) i_c	Sand boil, internally stable soils
	i_c < Terzaghi's (1922) i_c	Sand boil, internally unstable soils
	i_c > Terzaghi's (1922) i_c	Boiling sand, for all internally stable and many internally unstable soils
Ahlinhan and Achmus (2010)	i_{start} ~ Terzaghi's (1922) i_c	Suffusion, internally stable soils
	i_{start} ~ 1/3 to 1/5 Terzaghi's (1922)	Suffusion, internally unstable soils
Yang and Wang (2017)	i_c ~ Terzaghi's (1922) i_c	Sand boil, internally stable soils
	i_c ~ 1/2 Terzaghi's (1922) i_c	Sand boil, internally unstable soils

824 Once sand boils form, the hydraulic gradients required to transport sand vertically upwards is
825 expected to fall, because suffusion and heave, the precursors to sand boils, require higher
826 hydraulic gradients (compare Figure 4 with both Figure 3 and Terzaghi's (1922) i_c values of
827 1.16 and 1.22 described above). The interplay between hydraulic gradients and the formation
828 of preferential flow pathways (e.g., sand boil pipes), shown conceptually in Figure 5, indicates
829 that sand boil pipe formation in cohesive layers increases significantly the hydraulic gradients
830 in non-cohesive sediments, while reducing the hydraulic gradients acting within underlying or
831 overlying cohesive sediments. The same behaviour may not occur in homogeneous non-
832 cohesive sediment bodies, because preferential pathways do not necessarily modify hydraulic
833 gradients in undisturbed sediment, at least in theory (Figure 5A). Combining these concepts, it
834 would appear that sand boil pipes may be stable features where the source of sand and upward
835 flow are continuous, because hydraulic gradients may increase in sand bodies subsequent to
836 their formation, and yet sediment transport in pipes requires smaller hydraulic gradients than
837 that needed for suffusion and heave. However, the sequence of suffusion, heave, pipe formation
838 and sand boil occurrence, and the hydraulic gradients needed for each requires further
839 experimental analysis.
840
841 The subsurface sediment transport conceptual diagrams illustrated in Figure 1 can be extended
842 by considering the situation of relatively fine, non-cohesive sediment (e.g., silt, fine sand)
843 overlying coarse, non-cohesive sediment (e.g., medium or coarse sand). This is illustrated in
844 Figure 5c. Natural occurrences of this conceptual model include the widespread situation of
845 groundwater discharge through coarse bed sediments of the sea floor or terrestrial water bodies,
846 and the scenario of event-deposition of fine sediment due to floodwater sediment transport
847 (freshwater bodies) and littoral transport (ocean). The hydraulic gradients required to cause
848 suffusion, heave and/or sand movement through boil pipes are higher for coarser-grained

849 materials. Therefore, it is plausible that fine particles deposited over coarse-grained sediments
850 will be mobilized (i.e., they become fluidized) even though the underlying base material
851 remains stable. The likelihood of this phenomenon is increased by the effect of an upper, lower-
852 K layer on the hydraulic gradient distribution (Figure 5C), considering equations (15) and (16).
853 It follows that regions of groundwater discharge through coarse-grained materials in the beds
854 of surface water bodies may act to enhance littoral transport and suspended sediment loads
855 relative to regions where upwelling groundwater is absent. This is exemplified by field studies
856 of Duncan (1964) and Grant (1948) who demonstrate this phenomenon through the impact of
857 groundwater infiltration/exfiltration on swash sediment transport. Further research effort is
858 warranted to evaluate the occurrence and influence of the conceptual model of Figure 5c.
859
860 Whereas the analysis presented in this review adopts idealistic materials (e.g., uniform grain
861 sizes), Sherard et al. (1984) approximate $d_P = 0.11d_{15}$ for well-sorted materials. Assuming d_P
862 $= 0.11d_{15}$, it is possible to recalculate i_{suf} for natural (albeit well-sorted) materials. For example,
863 for test 9 (Table 5), i_{suf} is equal to 0.03 when $d_P = 0.11d_{15}$ is assumed, while minimum and
864 maximum values of i_{suf} are 0.13 and 0.28 with $d_P = 0.155d_{50}$ and $d_P = 0.414d_{50}$, respectively.
865 The corresponding measured value for i ("initial loss of fines" in Table 5) was reported by Wan
866 and Fell (2004) as 0.14. This shows that for natural materials, we expect that suffusion likely
867 involves significantly smaller ejected particles than those reported in the analysis for uniform
868 particles.
869
870 Our review finds significant knowledge gaps in the field of subsurface sediment transport. For
871 example, few field-scale studies have been undertaken to quantify suffusion, heave, hydraulic
872 fracturing and sand boil processes, despite that these features are encountered in a wide range
873 of situations. The contribution of subsurface sediment transport to littoral transport and the

874 suspension of sediment in open water bodies has not been previously assessed, with the
875 exception of swash-zone processes. The effect of vegetation on sand boil formation has not
876 been considered, even though the subsurface structures of roots are known to impart significant
877 geomechanical forces (e.g., Zhou and Qi, 2019). Another factor that may influence the
878 formation of voids (and perhaps preferential pathways) and subsurface sediment movement is
879 gas ebullition, which to the best of the authors' knowledge has not been studied previously in
880 the context of subsurface sediment transport, although the mechanisms leading to the formation
881 of bubbles in springs and wells have been explored (e.g., Agnew and Halihan, 2018). More
882 generally, the processes accompanying vertical subsurface sediment transport under
883 heterogeneous conditions is largely unstudied, including relationships between heterogeneities
884 and the formation of preferential flow paths. A rare attempt to manipulate subsurface sediment
885 transport was reported by de Louw et al. (2013), who attempted to seal sand boils in the
886 Haarlemmermeer and Noordplas Polders (The Netherlands). They found that the cessation of
887 flow in one boil led to rapid hydraulic gradient increase across the low-*K* confining unit, an
888 increase in flow in other boils, and the formation of new boils, to varying degrees in several
889 attempts at sealing saline boils in agricultural areas. These observations are consistent with
890 conceptual modelling undertaken as part of the current study (Figure 5), in relation to the effect
891 of preferential flow paths on low-*K* layers. Further research is warranted into intervening
892 engineering measures designed to modify situations involving subsurface sediment transport
893 through preferential flow paths. This is especially important in the face of projected sea-level
894 rise, which is likely to exacerbate these phenomena in the coming decades due to changing
895 head differences between the ocean and land. Additional evaluation of the importance of subsea
896 boils in submarine groundwater discharge (SGD) is also warranted given that the predominance
897 of SGD analyses neglect boil formation and flow (e.g., Moore, 2010; Konikow et al., 2013).
898 More generally, physics-based modelling of the various phenomena leading to the liberation

of sediment from the subsurface is warranted to unravel the influence of a wider range of factors than has been previously considered, and to build on the rudimentary functions based on simple force equilibria that are commonly adopted in practical applications (e.g., FEMA, 2015), and that are presented in the current article.

5. Conclusions

The current study evaluates different forms of vertical sediment transport in the subsurface through literature review and manipulation of previous theory. Subsurface sediment transport is a common phenomenon that is generally overlooked in the assessment of hydrological processes within catchments, sea and lake beds, and other areas within which groundwater discharge is expected. Rather, the primary foci of prior quantitative analyses of subsurface sediment transport are linked to engineered hydraulic structures. The various forms through which sediment may be liberated from the subsurface through groundwater discharge can be categorized into two groups: (1) suffusion, and (2) sand transport through preferential pathways. Sub-categories of (2) include: (a) point discharge caused by preferential flow through cohesive layers, (b) point discharge caused by preferential flow through non-cohesive sediment, and (c) dispersed discharge giving the appearance of boiling sand. Previous studies do not distinguish between the initial causes and driving processes associated with (a), (b) and (c), warranting further research effort.

Expressions are developed for the force balance at which upwards movement of subsurface sediment is expected to occur within each of the conceptual models described above, except the “boiling sand” category, which remains largely uncharacterised. Theories for the onset of sediment movement are described, based on parsimonious conceptual models and several

simplifying assumptions, and incorporating existing theory related to piping failure (e.g., of earthen structures), soil fluidization and soil heave. Groundwater flow in a selection of simple conceptual models is simulated using numerical modelling to demonstrate subsurface flow patterns associated with idealised boil structures, and critical changes to subsurface head distributions that arise with the onset of preferential flow or with the addition of overlying low-*K* layers. For example, the deposition of a layer of fine-grained material onto a region of groundwater discharge through coarse-grained sediment will create enhanced hydraulic gradients in the deposited material, increasing the likelihood that the fine-grained sediment is fluidized. Estimates of critical hydraulic gradients that lead to subsurface sediment transport are compared to available observations from previous laboratory experiments to test the validity of existing theory and the formulae developed within the current study. While suffusion appears more or less predictable using simple methods, the conditions leading to sand boils (and boiling sand) were poorly matched to theory.

The study of subsurface sediment transport requires additional effort to understand the mechanisms that lead to the liberation of sediment from preferential flow paths. While heave of cohesive sediments in a known precursor to sand boils, it is likely that heave is also required for preferential pathways to form in homogeneous, non-cohesive sediment bodies. Mismatch between theory and experimental results for the formation of boils in non-cohesive sediments perhaps indicates that heave in non-cohesive bodies requires hydraulic gradients that exceed those predicted by classic fluidization theory. This hypothesis should be tested using additional experimental work, which should also assess the occurrence of suffusion, heave and sand boils in heterogeneous media.

948 The results presented in this study are expected to have wide-ranging applications in terms of
949 sediment transport in coastal regions and surface water bodies, where groundwater discharge
950 occurs. While there is mismatch between theory and measurements when hydraulic gradients
951 are high, the simple theory of the current article nonetheless offers a framework for at least
952 initial estimates of the onset of sediment movement in discharging groundwater. Additionally,
953 the current theory may be extended to the study of the transport of other particulate matter,
954 including micro-plastics and biological particles, including faecal bacteria, which are released
955 from aquifers and may contaminate the drinking water supplies of surface storages (e.g., Frank
956 et al., 2018).
957
958 **Acknowledgments**
959
960 The authors are thankful for helpful discussions with Perry de Louw regarding boils in Dutch
961 polders, and Hongyu Qin for advice on aspects relating to geomechanics. Adrian Werner is the
962 recipient of an Australian Research Council Future Fellowship (project number
963 FT150100403). Amir Jazayeri is funded by the Australian Research Council (project numbers
964 FT150100403 and LP140100317).
965
966 **References**
967
968 Abdelhamid, Y., El Shamy, U. (2016). Pore-Scale Modeling of Fine-Particle Migration in
969 Granular Filters. *International Journal of Geomechanics*, 16(3), 04015086. doi:
970 10.1061/(ASCE)GM.1943-5622.0000592
971

Aboul Hosn, R., Sibille, L., Benahmed, N., Chareyre, B. (2018). A discrete numerical model involving partial fluid-solid coupling to describe suffusion effects in soils. *Computers and Geotechnics*, 95, 30-39. doi: 10.1016/j.compgeo.2017.11.006

Ahlinhan, M. F., Achmus, M. (2010). Experimental Investigation of Critical Hydraulic Gradients of Unstable Soils. *Scour and Erosion*, 5, 599-608. doi: 10.1061/41147(392)58

Ammerlaan, P. R. M. (2007). *Levees and levee evaluation, the Dutch and US practice compared* (M.Sc. thesis). Delft University of Technology, Delft.

Agnew, R. J., Halihan, T. (2018). Why Springs Bubble: A Framework for Gas Discharge in Groundwater. *Groundwater*, 56(6), 859-870. doi: 10.1111/gwat.12789

Arora, C., Kumar, B. P., Narayana, A. C. (2009). Influence of particle shape on drag coefficient for commonly occurring sandy particles in coastal areas. *Journal of Ocean and Climate: Science, Technology and Impacts*, 1(2), 99-112. doi: 10.1260/1759-3131.1.2.99

Baldock, T. E., Tomkins, M. R., Nielsen, P., Hughes, M. G. (2004). Settling velocity of sediments at high concentrations. *Coastal Engineering*, 51(1), 91-100. doi: 10.1016/j.coastaleng.2003.12.004

Bear, J. (1972). *Dynamics of fluids in porous media*. Amsterdam: Elsevier.

Bezuijen, A. (2015). *Critical vertical gradients in piping* (Report 1220088-003). Delft: Deltares.

Bezuijen, A., Vandenboer, K., van Beek, V., Robbins, B. (2019). Pressure drop in vertical pipes of sand boils. *European Conference on Soil Mechanics and Geotechnical Engineering*: *Proceeding of the XVII ECSMGE-2019.* Reykjavik, Iceland.

Bonelli, S., Nicot, F. (Eds.) (2013). *Erosion in Geomechanics Applied to Dams and Levees*. London: Wiley.

Bonelli, S., Fell, R., Benahmed, N. (2013). Concentrated Leak Erosion. In S. Bonelli & F. Nicot (Eds.), *Erosion in Geomechanics Applied to Dams and Levees* (pp. 271-341). London: Wiley. doi: 10.1002/9781118577165.ch4

Carman, P. C. (1937). Fluid flow through granular beds. *Transactions, Institution of Chemical Engineers (London)*, 15, 150-166.

Chang, D. S., Zhang, L. M. (2013). Extended internal stability criteria for soils under seepage. *Soils and Foundations*, 53, 569-583. doi: 10.1016/j.sandf.2013.06.008

Cheng, K., Wang, Y., Yang, Q. (2018). A semi-resolved CFD-DEM model for seepage-induced fine particle migration in gap-graded soils. *Computers and Geotechnics*, 100, 30-51. doi: 10.1016/j.compgeo.2018.04.004

Clift, R., Grace, J. R., Weber, M. E. (1978). *Bubbles, drops, and particles*. New York: Academic Press.

1022 Collins, R. E. (1961). *Flow of fluids through porous materials*. New York: Reinhold.
1023
1024 Decker, R. S., Dunnigan, L. P. (1977). Development and Use of the Soil Conservation Service
1025 Dispersion Test. In J. L. Sherard & R. S. Decker (Eds.), *Dispersive Clays, Related Piping, and*
1026 *Erosion in Geotechnical Projects* (pp. 94-109). West Conshohocken, PA: ASTM International.
1027 doi.org/10.1520/STP26982S
1028
1029 De Louw, P. G. B., Oude Essink, G. H. P., Stuyfzand, P. J., van der Zee, S. E. A. T. M. (2010).
1030 Upward groundwater flow in boils as the dominant mechanism of salinization in deep polders,
1031 The Netherlands. *Journal of Hydrology*, 394, 494-506. doi: 10.1016/j.jhydrol.2010.10.009
1032
1033 De Louw, P. G. B., Vandenbohede, A., Werner, A. D., Oude Essink, G. H. P. (2013). Natural
1034 saltwater upconing by preferential groundwater discharge through boils. *Journal of Hydrology*,
1035 490, 74-87. doi: 10.1016/j.jhydrol.2013.03.025
1036
1037 De Wit, J. M., Sellmeijer, J. B., Penning, A. (1981). Laboratory testing on piping. *Proceedings*
1038 *10th International Conference on Soil Mechanics and Foundation Engineering*. Stockholm,
1039 Sweden.
1040
1041 Duncan, J. R. (1964). The effects of water table and tidal cycle on swash-backwash sediment
1042 distribution and beach profile development. *Marine Geology*, 2(3),186-197. doi:
1043 10.1016/0025-3227(64)90039-8
1044
1045 Fancher, G. H., Lewis, J. A. (1933). Flow of simple fluids through porous materials. *Industrial*
1046 *and Engineering Chemistry*, 25(10), 1139-1147. doi: 10.1021/ie50286a020

Fannin, R.J., Moffat, R. (2006). Observations on internal stability of cohesionless soils. *Géotechnique*, 56 (7), 497-500. doi: 10.1680/geot.2006.56.7.497

Fannin, R. J., Slangen, P. (2014). On the distinct phenomena of suffusion and suffosion. *Géotechnique Letters*, 4(4), 289-294. doi: 10.1680/geolett.14.00051

Fell, R., Fry, J. (2013). State of The Art on the Likelihood of Internal Erosion of Dams and Levees by Means of Testing. In S. Bonelli. & F. Nicot (Eds.), *Erosion in Geomechanics Applied to Dams and Levees* (pp. 1-99). London: Wiley. doi: 10.1002/9781118577165.ch4

FEMA (2015). *Evaluation and Monitoring of Seepage and Internal Erosion, Interagency Committee on Dam Safety (ICODS)* (Report no. FEMA P-1032). Federal Emergency Management Agency. Retrieved from https://www.fema.gov/media-library/assets/documents/107639

Fitts, C. R. (2002). *Groundwater science*. London: Academic Press.

Fleshman, M. (2012). *Laboratory modelling of critical hydraulic conditions for the initiation of piping* (M.Sc. thesis). Utah State University, Logan.

Fleshman, M. S., Rice, J. D. (2014). Laboratory modeling of the mechanisms of piping erosion Initiation. *Journal of Geotechnical and Geoenvironmental Engineering*, 140(6), 04014017. doi: 10.1061/(ASCE)GT.1943-5606.0001106

Folk, R. L., Ward, W. C. (1957). Brazos River bar [Texas]; a study in the significance of grain size parameters. *Journal of Sedimentary Research*, 27(1), 3-26. doi: 10.1306/74D70646-2B21-11D7-8648000102C1865D

Frank, S., Goeppert, N., Goldscheider, N. (2018). Fluorescence-based multi-parameter approach to characterize dynamics of organic carbon, faecal bacteria and particles at alpine karst springs. *Science of The Total Environment*, 615, 1446-1459. doi: 10.1016/j.scitotenv.2017.09.095

Fujisawa, K., Murakami, A., Nishimura, S., Shuku, T. (2013). Relation between seepage force and velocity of sand particles during sand boiling. *Geotechnical Engineering Journal of the SEAGS & AGSSEA*, 44(2), 9-17.

Gibbs, R. J., Matthews, M. D., Link, D. A. (1971). The relationship between sphere size and settling velocity. *Journal of Sedimentary Petrology*, 41(1), 7-18. doi: 10.1306/74D721D0-2B21-11D7-8648000102C1865D

Glynn, M. E., Kuszmaul, J. (2010). *Prediction of piping erosion along middle Mississippi River levees -An empirical model* (Report no. ERDC/ GSL TR-04-12). Washington, DC: U.S. Army Corps of Engineers.

Grant, U. S. (1948). Influence of the water table on beach aggradation and degradation. *Journal of Marine Research*, 7, 655-660.

Graton, L. C., Fraser, H. J. (1935). Systematic packing of spheres: with particular relation to porosity and permeability. *The Journal of Geology*, 43(8), 785-909.

Gray, W. A. (1968). *The Packing of solid particles*, London: Chapman and Hill Ltd.

Gupta, S. C., Larson, W. E. (1979). A Model for Predicting Packing Density of Soils Using Particle-Size Distribution. *Soil Science Society of America Journal*, 43(4), 758-764. doi: 10.2136/sssaj1979.03615995004300040028x

Hagen, G. H. L. (1839). Ueber die Bewegung des Wassers in engen cylindrischen Röhren. *Annalen der Physik und Chemie*, 46, 423-442. doi: 10.1002/andp.18391220304

Hagerty, D. J. (1991). Piping/Sapping Erosion. I: Basic Considerations. *Journal of Hydraulic Engineering*, 117(8), 991-1008. doi: 10.1061/(ASCE)0733-9429(1991)117:8(991)

Hagerty, D. J. (1992). *Identification of Piping and Sapping Erosion of Streambanks* (Contract Report HL-92-1). Washington, DC: U.S. Army Corps of Engineers.

Harbaugh, A. W. (2005). *MODFLOW-2005: the U.S. Geological Survey modular groundwater model - the ground-water flow process*. U.S. Geological Survey Techniques and Methods 6-A16. Reston. doi: 10.3133/tm6A16

Heywood, H. (1962). Uniform and non-uniform motion of particles in fluids. *Institute of Chemical Engineering: Proceeding of the Symposium on the Interaction between Fluid and Particles*. London, UK.

Indraratna, B., Nguyen, V. T., Rujikiatkamjorn, C. (2011). Assessing the potential of internal erosion and suffusion of granular soils. *Journal of Geotechnical and Geoenvironmental Engineering*, 137 (5), 550-554. doi: 10.1061/(ASCE)GT.1943-5606.0000447

Jones, J. A. A. (1981). *The Nature of Soil Piping: A Review of Research. British Geomorphological Research Group Research Monograph 3*. Norwich: GeoBooks.

Kamphuis, J. W. (1974). Determination of sand roughness for fixed beds. *Journal of Hydraulic Research*, 12(2), 193-203. doi: 10.1080/00221687409499737

Kenney, T. C., Lau, D. (1985). Internal stability of granular filters. *Canadian Geotechnical Journal*, 22(2), 215-225. doi: 10.1139/t85-029

Knappett, J. A., Craig, R. F. (2012). *Craig's soil mechanics* (8th ed.). New York: Spon Press.

Konikow, L. F., Akhaan, M., Langevin, C. D., Michael, H. A., Sawyer, A. H. (2013). Seawater circulation in sediments driven by interactions between seabed topography and fluid density. *Water Resources Research*, 49, 1386-1399. doi: 10.1002/wrcr.20121

Kovacs, G. (1981). *Developments in water science-seepage hydraulics*. Amsterdam: Elsevier.

Kozeny, J. (1927). Ueber kapillare Leitung des Wassers im Boden. Sitzungsber Akad, Wiss., Wien, 136(2a), 271-306.

Lamb, H. (1932). *Hydrodynamics* (6th ed.). London: Cambridge University Press.

Li, Y., Craven, J., Schweig, E. S., Obermeier, S. F. (1996). Sand boils induced by the 1993 Mississippi River flood: Could they one day be misinterpreted as earthquake induced liquefaction? *Geology*, 24(2), 171-174. doi: 10.1130/0091-7613(1996)024<0171:SBIBTM>2.3.CO;2

Liang, Y., Zeng, C., Wang, J. -J., Liu, M. -W., Yeh, T. -C. J., Zha, Y. -Y. (2017). Constant gradient erosion apparatus for appraisal of piping behavior in upward seepage flow. *Geotechnical Testing Journal*, 40(4), 630-642. doi: 10.1520/GTJ20150282

Madhav, G. V., Chhabra, R. P. (1995). Drag on non-spherical particles in viscous fluids. *International Journal of Mineral Processing*, 43(1-2), 15-29. doi: 10.1016/0301-7516(94)00038-2

Mansur, C. I., Postol, G., Salley, J. R. (2000). Performance of relief well systems along Mississippi River levees. *Journal of Geotechnical and Geoenvironmental Engineering*, 126(8), 727-738. doi: 10.1061/(ASCE)1090-0241(2000)126:8(727)

Miesel, D. (1978). Rückschreitende Erosion unter Bindiger Deckschicht, Vorträge der Baugrundtagung, Berlin, Deutsche Gesellschaft für Erd-und Grundbau E. V.

Moffat, R., Fannin, R. J., Garner, S. J. (2011). Spatial and temporal progression of internal erosion in cohesionless soil. *Canadian Geotechnical Journal*, 48(3), 399-412. doi: 10.1139/T10-071

Moore, W. S. (2010). The Effect of Submarine Groundwater Discharge on the Ocean. *Annual Review of Marine Science*, 2, 59-88. doi: 10.1146/annurev-marine-120308-081019

Moriasi, D., Arnold, J., Van Liew, M., Bingner, R., Harmel, R., Veith, T. (2007). Model evaluation guidelines for systematic quantification of accuracy in watershed simulations. *Transactions of the ASABE*, 50(3), 885-900. doi: 10.13031/2013.23153

Muller-Kirchenbauer, H. (1978). Zum Zeitlichen Verlauf der Rückschreitenden Erosion in Geschichtetem Untergrund unter Dämmen und Stauanlagen, Beitrag zum Talsperrensymposium, München.

Nakayama, Y. (1999). *Introduction to Fluid Mechanics*. Oxford: Butterworth-Heinemann.

Petrula, L., Hala, M., Říha, J. (2019). Uncertainty in Determining the Critical Hydraulic Gradient of Uniform Glass Beads. In S. Bonelli, C. Jommi & D. Sterpi (Eds). *Internal Erosion in Earthdams, Dikes and Levees: Proceeding of EWG-IE 26th Annual Meeting 2018*. *Lecture Notes in Civil Engineering*. Cham: Springer. doi: 10.1007/978-3-319-99423-9_8

Poiseuille, J. L. M. (1841). Recherches experimentales sur Ie mouvement des liquides dans les tubes de tres petits diametres, IV. Influence de la temperature sur la quantite de liquide qui traverse les tubes de tres petits diametres, Comptes rendus de l'Academie des Sciences, 12, 11215.

1195 Prandtl, L., Tietjens, O. G. (1934). *Applied hydro- and aeromechanics*. New York: McGraw-
1196 Hill Book Co.
1197
1198 Richards, K. S., Reddy, K. R. (2007). Critical appraisal of piping phenomena in earth dams.
1199 *Bulletin of Engineering Geology and the Environment*, 66, 381-402. doi: 10.1007/s10064-007-
1200 0095-0
1201
1202 Richardson, J. F., Zaki, W. N. (1954). Sedimentation and fluidisation: Part 1. *Chemical*
1203 *Engineering Research and Design*, 75(Suppl.), S82-S100. doi: 10.1016/S0263-
1204 8762(97)80006-8
1205
1206 Robbins, B. A., Stephens, I. J., Van Beek, V. M., Koelewijn, A. R., Bezuijen, A. (2019). Field
1207 measurements of sand boil hydraulics. *Géotechnique*,1-8. doi: 10.1680/jgeot.18.P.151
1208
1209 Schmertmann, J. H. (2000). The non-filter factor of safety against piping through sands. In F.
1210 Silva & E. Kavazanjian (Eds.), *Judgment and Innovation. Geotechnical Special Publication*
1211 (pp. 65-132). Reston: American Society of Civil Engineers.
1212
1213 Schmertmann, J. H. (2015). Discussion of "Laboratory Modeling of the Mechanisms of Piping
1214 Erosion Initiation" by Mandie S. Fleshman and John D. Rice. *Journal of Geotechnical and*
1215 *Geoenvironmental Engineering*, 141(8), 07015015. doi: 10.1061/(ASCE)GT.1943-
1216 5606.0001309
1217
1218 Sellmeijer, J. B. (1988). *On the Mechanism of Piping under Impervious Structures* (Ph.D.
1219 thesis). Delft University of Technology, Delft.

Sherard, J. L., Dunnigan, L. P., Talbot, J. R. (1984). Basic properties of sand and gravel filters. *Journal of Geotechnical Engineering*, 110(6), 684-700. doi: 10.1061/(ASCE)0733-9410(1984)110:6(684)

Silvis, F. (1991). Verificatie piping model: proeven in de deltagoot (in Dutch), Grondmechanica Delft, The Netherlands.

Skempton, A. W., Brogan, J. M. (1994). Experiments on piping in sandy gravels. *Geotechnique*, 44(3), 449-460. doi: 10.1680/geot.1994.44.3.449

Sterpi, D. (2003). Effects of the erosion and transport of fine particles due to seepage flow. *International Journal of Geomechanics*, 3(1), 111-122. doi:10.1061/(ASCE)1532-3641(2003)3:1(111)

TACFD (1999). *Technical Report on Sand Boils (Piping)*. Delft: Technical Advisory Committee on Flood Defences.

Terzaghi, K. (1922). Der Grundbruch an Stauwerken und seine Verhutung (The failure of dams by piping and its prevention). *Die Wasserkraft*, 17, 445-449. Reprinted in (1960) *From theory to practice in soil mechanics*. New York: Wiley.

Townsend, F. C. D., Bloomquist, D., Shiau, J. M., Martinez, R. Rubin, H. (1988). *Analytical and Experimental Investigation of Piping and Filter Design for Sands, Report to the Bureau of Reclamation.* Gainesville, Florida: Department of Civil Engineering, University of Florida.

Tran-Cong, S., Gay, M., Michaelides, E. E. (2004). Drag coefficients of irregularly shaped particles. *Powder Technology*, 139(1), 21-32. doi: 10.1016/j.powtec.2003.10.002

Turnbull, W. J., Mansur, C. I. (1959). Investigation of underseepage-Mississippi River levees. *Journal of the Soil Mechanics and Foundations Division*, 85(4), 41-94.

USACE (1956). *Investigation of underseepage and its control, Lower Mississippi River Levees, Volume I; Waterways Experiment Station*. Vicksburg, Mississippi: U.S. Army Corps of Engineers.

USACE (2005). *Design guidance for levee under-seepage*. Washington, DC: U.S. Army Corps of Engineers.

Van Beek, V. M., Knoeff, H., Sellmeijer, H. (2011). Observations on the process of backward erosion piping in small-, medium- and full-scale experiments. *European Journal of Environmental and Civil Engineering*, 15(8), 1115-1137. doi: 10.1080/19648189.2011.9714844

Van Beek, V. M., van Bezuijen, A., Sellmeijer, H. (2013). Backward erosion piping. In S. Bonelli (Ed.). *Erosion in Geomechanics Applied to Dams and Levees* (pp. 193-269). London: Wiley. doi: 10.1002/9781118577165.ch3

Wadell, H. (1933). Sphericity and roundness of rock particles. *The Journal of Geology*, 41(3), 310–331. doi: 10.1086/624040

Wan, C. F., Fell, R. (2004). *Experimental investigation of internal erosion by the process of suffusion in embankment dams and their foundations* (UNICIV REPORT No. R-429). Sydney: University of New South Wales.

Wan, C. F., Fell, R. (2008). Assessing the potential of internal instability and suffusion in embankment dams and their foundations. *Journal of Geotechnical and Geoenvironmental Engineering*, 134 (3), 401-407. doi: 10.1061/(ASCE)1090-0241(2008)134:3(401)

Ward, J. C. (1964). Turbulent flow in porous media. *Journal of the Hydraulics Division*, 90(5), 1-12.

Wentworth, C. (1922). A Scale of Grade and Class Terms for Clastic Sediments. *The Journal of Geology*, 30(5), 377-392.

White, H. E., Walton, S. F. (1937) Particle packing and particle shape. *Journal of the American Ceramic Soci*ety, 20(1-12), 155-166. doi: 10.1111/j.1151-2916.1937.tb19882.x

Worman, A., Olafsdottir, R. (1992). Erosion in a granular medium interface. *Journal of Hydraulic Research*, 30(5), 639-655. doi: 10.1080/00221689209498885

Yang, K. -H., Wang, J. -Y. (2017). Experiment and statistical assessment on piping failures in soils with different gradations. *Marine Georesources and Geotechnology* 35(4), 512-527. doi: 10.1080/1064119X.2016.1213338

Yao, Q., Xie, J., Sun, D., Zhao, J. (2009). *Sino-Dutch Cooperation Project-data collection of dike breach cases of China*. Beijing: China Institute of Water Resources and Hydropower Research.

Yap, H. (1981). *Fluidisatieproeven op Strandzand. Laboratorium voor Grondmechanica Delft* (Report CO-220884). Delft (in Dutch).

Zeng, Z., Grigg, R. J. (2006). A criterion for non-Darcy flow in porous media. *Transport in Porous Media*, 63(1), 57-69. doi: 10.1007/s11242-005-2720-3

Zhou, W. -H., Qi, X. -H. (2019). Root cohesion estimation of riparian trees based on model uncertainty characterization. *Journal of Materials in Civil Engineering*, 31(2), 04018389. doi: 10.1061/(ASCE)MT.1943-5533.0002600

Zhou, Z. Y., Kuang, S. B., Chu, K. W., Yu, A. B. (2010) Discrete particle simulation of particle-fluid flow: model formulations and their applicability. *Journal of Fluid Mechanics*, 661, 482-510. doi: 10.1017/S002211201000306X